Dissipative quantum systems with a potential barrier. II. Dynamics near the barrier top

Joachim Ankerhold and Hermann Grabert
Fakultät für Physik der Albert-Ludwigs-Universität, Hermann-Herder Strasse 3, D-79104 Freiburg im Breisgau, Germany
(Received 29 March 1995; revised manuscript received 14 June 1995)

We study the real time dynamics of a quantum system with a potential barrier coupled to a heat-bath environment. The time evolution of the density matrix starting from a general initial state is evaluated explicitly in the semiclassical approximation. As the temperature is decreased below a critical temperature T_c, large quantum fluctuations render the harmonic approximation near the barrier top insufficient and a caustic arises. As a consequence, anharmonicities of the potential become essential even in the close vicinity of the barrier top and the semiclassical density matrix has to be evaluated beyond the Gaussian approximation. The range of validity with respect to temperature and time of the semiclassical analytical results is discussed in detail. We illustrate the outcome of the theory with an explicit example.

PACS number(s): 05.40.+j, 03.65.Sq, 82.20.Db

I. INTRODUCTION

In most problems of barrier penetration in physics and chemistry the reaction coordinate describing the transition across the barrier interacts with a large number of microscopic degrees of freedom. Hence the theoretical description has to incorporate the effects of a heat bath environment. Although this problem has been studied extensively in the past decade [1], an approach to dissipative barrier transmission processes without any *ad hoc* assumptions is still not available in the quantum regime. In an earlier article [2], which is referred to as I henceforth, we have given a general framework to investigate the problem of dissipative barrier penetration on the basis of a dynamical theory. The method is based on the path integral description of dissipative quantum systems introduced by Feynman and co-workers [3,4]. These techniques have been employed by Caldeira and Leggett [5] to treat barrier penetration problems and extended to a wider class of useful initial conditions by Grabert *et al.* [6]. In I we applied the theory of dissipative quantum mechanics [6,7] to a system with a potential barrier, the height of which is large compared to other relevant energy scales. Then a semiclassical evaluation of the path integrals determining the time-dependent density matrix is adequate. We have shown explicitly that for high enough temperatures, where the barrier is crossed primarily by thermally activated processes, the resulting evolution law for the density matrix allows for a nonequilibrium quasistationary flux state. In the temperature range studied in I the flux state is only affected by the harmonic part of the barrier potential and the resulting barrier penetration rate was found to coincide with earlier results on quantum corrections to thermally activated processes derived by thermodynamic methods [8]. In the present article we extend the theory to the temperature region where quantum tunneling becomes essential.

Within the path integral approach the position representation of the time-dependent density matrix is given as a threefold path integral where two path integrals are in real time and one is in imaginary time. As discussed in detail in I, when the temperature is lowered the harmonic approximation for the barrier potential causes specific divergencies of the imaginary time path integral. Well known as the problem of caustics [9], these divergencies are an artifact of the harmonic approximation of the potential. As a consequence, the evaluation of the imaginary time path integral in the Gaussian semiclassical approximation breaks down near the caustic and anharmonicities of the potential must be taken into account even for coordinates near the barrier top. This problem is independent of damping and occurs already in the semiclassical evaluation of the equilibrium density matrix of a system with barrier potential [10,11].

To extend the dynamical theory of quantum mechanical barrier transmission presented in I to lower temperatures, one has to determine the time evolution of the density matrix for temperatures near T_c where the Gaussian semiclassical approximation for the density matrix breaks down. This is done in the present article for a general anharmonic and symmetric barrier potential. On one hand, the analytical results derived can be used to investigate the dynamics near the barrier top for a wide class of nonequilibrium initial states; on the other hand, they can be applied to determine the nonequilibrium stationary flux state near T_c, which is planned for a subsequent work.

The article is organized as follows. In Sec. II we specify the problem introducing the barrier potential and the expansion parameters for the semiclassical approximation. The explicit evaluation of the minimal action paths is performed in Secs. III and IV. In Sec. V the corresponding minimal action is discussed. The contribution of the quantum fluctuations about the minimal action paths is determined in Sec. VI, leading to the semiclassical time-dependent density matrix. Finally, in Sec. VII we illustrate our results with an explicit example and

present our conclusions. Most of the results of the article are also included in [12].

II. FORMULATION OF THE PROBLEM

As shown in detail in [6] the position representation of the time-dependent reduced density matrix of a dissipative quantum system can be written as

$$\rho(x_f,r_f,t) = \int dx_i dr_i d\bar{q}\, d\bar{q}'\, J(x_f,r_f,t,x_i,r_i,\bar{q},\bar{q}') \times\lambda(x_i,r_i,\bar{q},\bar{q}'). \quad (1)$$

Here $J(x_f,r_f,t,x_i,r_i,\bar{q},\bar{q}')$ denotes the propagating function given as a three-fold path integral where two path integrals are in real time and one is in imaginary time. The preparation function $\lambda(x_i,r_i,\bar{q},\bar{q}')$ describes the deviation from thermal equilibrium in the initial state

$$\rho(x_f,r_f,0) = \int d\bar{q}\, d\bar{q}'\, \lambda(x_f,r_f,\bar{q},\bar{q}')\rho_\beta(\bar{q},\bar{q}'), \quad (2)$$

where $\rho_\beta = \mathrm{tr}_R(W_\beta)$ in which W_β is the equilibrium density matrix of the entire system.

In the following, we consider the dynamics of systems in a potential field $V(q)$ that has a barrier. In particular, we study the semiclassical approximation of the propagating function for coordinates near the barrier top.

A. Barrier potential and expansion parameters

Assuming that the barrier top is at $q = 0$ and $V(0) = 0$, the general form of a symmetric barrier potential reads

$$V(q) = -\frac{1}{2}M\omega_0^2 q^2\left[1 - \sum_{k=2}^{\infty}\frac{c_{2k}}{k}\left(\frac{q}{q_a}\right)^{2k-2} q^{2k-2}\right]. \quad (3)$$

Here the c_{2k} are dimensionless coefficients. We assume $c_4 > 0$ so that the barrier potential becomes broader than its harmonic approximation at lower energies. q_a is a characteristic length indicating a typical distance from the barrier top at which anharmonic terms of the potential becomes essential. For small $|q| \ll q_a$, the barrier potential is harmonic with frequency ω_0. For the following discussion it is convenient to introduce a second length scale q_b, which characterizes the barrier region within which we want to determine the time evolution. The barrier region is chosen sufficiently small so that

$$\xi = q_b/q_a \quad (4)$$

is a small dimensionless parameter.

Of course, for an anharmonic potential field, the three-fold path integral defining the propagating function in (1) cannot be evaluated exactly. However, when the quantum mechanical ground state in the inverted barrier potential is only weakly affected by anharmonicities of the potential, a semiclassical approximation of the propagating function suffices for coordinates near the barrier top. In I we introduced $q_0 = \sqrt{\hbar/2M\omega_0}$ as a natural quantum mechanical length scale that is the variance of the coordinate in the ground state of a harmonic oscillator with oscillation frequency ω_0. Hence a semiclassical evaluation of the path integral is sufficient if

$$\epsilon = q_0/q_a \quad (5)$$

is a small dimensionless parameter. Within the semiclassical approximation, we first consider the classical motion in the anharmonic potential. Afterward, the quantum fluctuations about the classical paths are determined. Since neither the classical nor the quantum dynamics can be solved exactly, both the small parameter ξ for the classical motion and the small parameter ϵ for the quantum fluctuations will serve as expansion parameters to evaluate the density matrix (1) analytically for coordinates near the barrier top.

This calculation becomes more transparent if we introduce a *dimensionless formulation.* In the following, all coordinates are measured in units of q_b, all frequencies in units of ω_0, and all times in units of $1/\omega_0$. According to (I26) [13], the propagating function in (1) then reads, in terms of the sum and difference coordinates x and r defined in (I22),

$$J(x_f,r_f,t,x_i,r_i,\bar{q},\bar{q}') = \frac{1}{Z}\frac{\xi^3}{\epsilon^3}\int \mathcal{D}x\mathcal{D}r\mathcal{D}\bar{q}\,\exp\left[\frac{i}{2}\frac{\xi^2}{\epsilon^2}\Sigma[x,r,\bar{q}]\right], \quad (6)$$

where the path integral is over all paths $x(s)$ and $r(s)$, $0 \le s \le t$, in real time with

$$x(0) = x_i,\ r(0) = r_i,\ x(t) = x_f,\ r(t) = r_f$$

and over all paths $\bar{q}(\sigma)$, $0 \le \sigma \le \theta$, in imaginary time with $\bar{q}(0) = \bar{q}'$ and $\bar{q}(\theta) = \bar{q}$. Here $\theta = \hbar\beta\omega_0$ is the dimensionless inverse temperature and, according to (I28), the effective action $\Sigma[x,r,\bar{q}]$ is given by

$$\Sigma[x,r,\bar{q}] = i\int_0^\theta d\sigma\left[\frac{1}{2}\dot{\bar{q}}^2 + V(\bar{q}) + \frac{1}{2}\int_0^\theta d\sigma' k(\sigma-\sigma')\,\bar{q}(\sigma)\bar{q}(\sigma')\right] + \int_0^\theta d\sigma\int_0^t ds K^*(s-i\sigma)\,\bar{q}(\sigma)x(s)$$
$$+\int_0^t ds\,[\dot{x}\dot{r} - V(r+x/2) + V(r-x/2) - r_i\gamma(s)x(s)]$$
$$-\int_0^t ds\left[\int_0^s ds'\gamma(s-s')\,x(s)\dot{r}(s') - \frac{i}{2}\int_0^t ds' K'(s-s')\,x(s)x(s')\right]. \quad (7)$$

Here the asterisk denotes complex conjugation and the kernel $K(s-i\sigma)$ is specified in (I29). The dimensionless potential field is given by

$$V(q) = -\frac{1}{2}q^2\left(1-\sum_{k=2}^{\infty}\frac{c_{2k}}{k}\xi^{2k-2}\,q^{2k-2}\right). \tag{8}$$

We mention that, because within the harmonic approximation the classical equations of motion can be solved exactly, there was no need to introduce a classical expansion parameter ξ in I. Formally, we recover the dimensionless formulation in I by setting $\xi=\epsilon$. Furthermore, we note that the relevant quantum fluctuations give a contribution to the full action Σ of order 1 (i.e., of order $\hbar$ in dimensional units). Hence the semiclassical expansion is consistent only when the classical action as an expansion in terms of ξ is also determined at least to order 1.

B. Critical temperature

For high temperatures the anharmonic terms in the potential (8) give only small corrections and a simple semiclassical approximation with Gaussian fluctuations is appropriate, as shown in I. However, the harmonic approximation breaks down and anharmonicities become essential even for coordinates near the barrier top when the temperature is lowered. Near a critical temperature T_c determined by

$$\Lambda(\theta_c) = -\frac{1}{\theta}+\frac{2}{\theta}\sum_{n=1}^{\infty}\frac{1}{\nu_n^2-1+\nu_n\hat{\gamma}(\nu_n)}\bigg|_{\theta=\theta_c} = 0, \tag{9}$$

the propagating function diverges within the harmonic approximation. Here $\nu_n = 2\pi n/\theta$ are the dimensionless Matsubara frequencies and $\hat{\gamma}(z)$ denotes the Laplace transform of the macroscopic damping kernel $\gamma(s)$. For vanishing damping one has $\Lambda = -\frac{1}{2}\cot(\theta/2)$ and therefore $\theta_c=\pi$, i.e., $T_c = \hbar\omega_0/\pi k_B$ in dimensional units. This divergence corresponds to the problem of caustics for a harmonic oscillator [9,10]. Since the caustics are an artifact of the harmonic approximation, the temperature region near and below T_c requires explicit account of the anharmonicities of the barrier potential.

In the following, we extend the investigation in I and evaluate the density matrix $\rho(x_f,r_f,t)$ in a semiclassical approximation near T_c and for coordinates near the barrier top. Hence we are interested in dimensional coordinates q and q' of order q_b or smaller, that is, in dimensionless coordinates x_f and r_f of order 1 or smaller. In the worst case the density matrix $\rho(x_f,r_f,t)$ could be affected by trajectories starting at $t=0$ in the nonlinear range of the potential, that is, near initial dimensional coordinates of order q_a. In dimensionless units x_i, r_i, $\bar{q}$, and $\bar{q}'$ would then be of order $1/\xi$. Now, from I we know that well above T_c and within a large time domain, excluding, however, extremely long times, the main contribution to $\rho(x_f,r_f,t)$ comes from trajectories with x_i, r_i, $\bar{q}$, and $\bar{q}'$ of order 1 or smaller. For lower temperatures the range of initial coordinates that are relevant for the density matrix increases and near T_c the coordinates can be restricted to be at most of order 1 only for small times. However, we are primarily interested in the behavior of the density matrix for long times. In a subsequent paper we plan to show that near and above T_c, a semiclassical approximation for initial coordinates that are of order $\xi^{-1/4}$ or smaller suffices to determine the behavior of the density matrix in the barrier region on the time scale of the quasistationary nonequilibrium flux state. Hence we shall seek in this article solutions of the equations of motions for end points of order $\xi^{-1/4}$.

In Sec. III we first determine perturbatively the extremal imaginary time path for temperatures near T_c. This requires some care since near T_c, the imaginary time path is affected strongly by anharmonicities and a simple expansion about the path in the harmonic approximation fails. Subsequently, in Secs. IV and V the extremal real time paths and the minimal effective action are evaluated perturbatively. Thereby, we use ξ as an expansion parameter. For the range of end points considered here, the minimal action paths are affected only by a finite number of anharmonic terms in the expansion (8) of the barrier potential, which is the reason why we can obtain analytic results.

III. EXTREMAL IMAGINARY TIME PATH

In this section we solve the equation of motion for the extremal path in imaginary time for small ξ.

A. Marginal mode

The equations of motion for the extremal paths of the effective action in the propagating function are given by (I41)–(I43). In particular, the minimal action path in imaginary times obeys the equation of motion

$$\ddot{\bar{q}} - \int_0^{\theta} d\sigma'\, k(\sigma-\sigma')\bar{q}(\sigma') - \frac{dV(\bar{q})}{d\bar{q}} = -i\int_0^t ds K^*(s-i\sigma)x(s), \tag{10}$$

where $\bar{q}(0)=\bar{q}'$ and $\bar{q}(\theta)=\bar{q}$. The inhomogeneity on the right-hand side couples $\bar{q}(\sigma)$ to the real time motion.

For high temperatures (10) was solved in I using the Fourier expansion

$$\bar{q}(\sigma) = \frac{1}{\theta}\sum_{n=-\infty}^{\infty} q_n \exp\left(i\nu_n\sigma\right). \tag{11}$$

However, as mentioned above, when the temperature is lowered, that is, the dimensionless inverse temperature θ is increased, the Fourier coefficients q_n diverge for a purely harmonic barrier when θ_c is approached. For vanishing damping and a weakly anharmonic potential it can been shown [10] that one may choose an appropri-

ate Fourier expansion of the extremal action path where only one Fourier mode amplitude grows near θ_c and then saturates at a finite value due to the anharmonicities of the potential. Accordingly, to determine the imaginary time path $\bar{q}(\sigma)$ near θ_c for finite damping, we first have to identify the marginal direction in function space along which the solution of (10) within the harmonic approximation grows for $\theta \to \theta_c$. From the solution (I57), which we refer to as the "harmonic path" henceforth, we obtain

$$\lim_{\theta\to\theta_c} \Lambda\bar{q}(\sigma) = \frac{\bar{b}}{\theta} \sum_{n=-\infty}^{\infty} u_n \exp(i\nu_n\sigma)\Big|_{\theta=\theta_c}, \tag{12}$$

with the abbreviation

$$u_n = \left[\nu_n^2 - 1 + |\nu_n|\hat{\gamma}(|\nu_n|)\right]^{-1} \tag{13}$$

and where, according to (I56),

$$\bar{b} = \bar{r} - \frac{i}{\theta} \sum_{n=-\infty}^{\infty} u_n\, g_n[x(s)] \tag{14}$$

remains finite for vanishing Λ. At $\theta = \theta_c$ the right-hand side of (12) vanishes at the boundaries of the time interval $[0,\theta]$. The marginal direction $\phi(\sigma)$ in function space, which satisfies the boundary condition $\phi(0) = \phi(\theta) = 0$ also for $\theta \neq \theta_c$, is then obtained as

$$\phi(\sigma) = -\Lambda + \frac{1}{\theta} \sum_{n=-\infty}^{\infty} u_n \exp(i\nu_n\sigma). \tag{15}$$

For vanishing damping we have

$$\lim_{\gamma\to 0} \lim_{\theta\to\theta_c} \phi(\sigma) = -\frac{1}{2}\sin(\sigma),\ \sigma \in [0,\theta], \tag{16}$$

which coincides with our earlier result [10]. In view of (16) it is convenient to use the Fourier expansion

$$\bar{q}(\sigma) = \frac{1}{\theta} \sum_{k=1}^{\infty} Q_k \sin\left(\frac{\nu_k}{2}\sigma\right) \tag{17}$$

to determine $\bar{q}(\sigma)$ near θ_c. This series continues the path outside $[0,\theta]$ as an antisymmetric and periodic path with period 2θ leading to jump singularities in $\bar{q}(\sigma)$ at the end points of the time interval. The singularities are completely determined by the boundary conditions of the periodically continued path $\bar{q}(\sigma)$, i.e.,

$$\begin{aligned} \bar{q}(0^+) - \bar{q}(0^-) &= 2\bar{q}', \\ \bar{q}(\theta^+) - \bar{q}(\theta^-) &= -2\bar{q}. \end{aligned} \tag{18}$$

The matrix that transforms between the basis $\{\exp(i\nu_n\sigma)\}_{n=-\infty}^{+\infty}$ and the basis $\{\sin(\nu_k\sigma/2)\}_{k=1}^{\infty}$ has the coefficients

$$U_{k,n} = \frac{2}{\theta}\int_0^\theta d\sigma \sin\left(\frac{\nu_k}{2}\sigma\right)\exp(i\nu_n\sigma). \tag{19}$$

For k even, one simply has

$$U_{2l,n} = i\,\delta_{l,|n|}\ \mathrm{sgn}(n), \quad l = 1,2,3,\ldots, \tag{20}$$

while for k odd,

$$U_{2l+1,n} = \frac{4}{\pi}\frac{2l+1}{(2l+1)^2 - (2n)^2}, \quad l = 0,1,2,\ldots. \tag{21}$$

Clearly, up to a normalization constant the matrix $U_{k,n}$ is unitary. For convenience, the normalization in (21) has been chosen so that

$$\sum_{n=-\infty}^{\infty} U_{2l+1,n}U_{2l'+1,n} = 2\delta_{l,l'}. \tag{22}$$

Of course, in the time interval $(0,\theta)$ the Fourier expansions (11) and (17) coincide. From (12) the marginal mode is found to read

$$\begin{aligned} \phi(\sigma) &= \frac{1}{\theta}\sum_{l=0}^{\infty}\sum_{n=-\infty}^{\infty} U_{2l+1,n}\, u_n \sin\left(\frac{\nu_{2l+1}}{2}\sigma\right) \\ &\quad -\frac{4\Lambda}{\pi}\sum_{l=0}^{\infty}\frac{1}{2l+1}\sin\left(\frac{\nu_{2l+1}}{2}\sigma\right) \\ &= \frac{1}{\theta}\sum_{l=0}^{\infty}\sum_{n=-\infty}^{\infty}\left(\frac{2n}{2l+1}\right)^2 U_{2l+1,n}\, u_n \sin\left(\frac{\nu_{2l+1}}{2}\sigma\right), \end{aligned} \tag{23}$$

which gives the marginal mode in the representation (17). Here the second sum in the intermediate result is the Fourier representation of the constant part in (15) with a discontinuity at $\sigma = 0$

$$\lim_{\sigma\to 0\pm}\frac{4\Lambda}{\pi}\sum_{l=0}^{\infty}\frac{1}{2l+1}\sin\left(\frac{\nu_{2l+1}}{2}\sigma\right) = \pm\Lambda. \tag{24}$$

By the use of (20) and (21), the imaginary time path (I57) in the harmonic approximation may be written as

$$\begin{aligned} \bar{q}(\sigma) &= \frac{1}{\theta}\sum_{l=0}^{\infty} u_l\left\{-2\nu_l\bar{x} - 2f_l[x(s)]\right\}\sin(\nu_l\sigma) \\ &\quad + \frac{\bar{b}}{\Lambda}\phi(\sigma) + \hat{q}(\sigma). \end{aligned} \tag{25}$$

Here $\bar{x} = \bar{q} - \bar{q}'$ and

$$\begin{aligned} \hat{q}(\sigma) &= \frac{i}{\theta}\sum_{l=0}^{\infty}\sum_{n=-\infty}^{\infty}\left(\frac{2n}{2l+1}\right)^2 U_{2l+1,n}\, u_n g_n[x(s)] \\ &\quad \times \sin\left(\frac{\nu_{2l+1}}{2}\sigma\right) + \frac{4\bar{r}}{\pi}\sum_{l=0}^{\infty}\frac{1}{2l+1}\sin\left(\frac{\nu_{2l+1}}{2}\sigma\right) \end{aligned} \tag{26}$$

collects terms in the subspace $\{\sin(\nu_{2l+1}\sigma/2)\}_{l=0}^{\infty}$ that remain of order 1 or smaller near θ_c. Furthermore, the functionals

$$f_n[x(s)] = \int_0^t ds\, f_n(s)x(s) \tag{27}$$

and

$$g_n[x(s)] = \int_0^t ds\, g_n(s)x(s) \tag{28}$$

describe the coupling to the real time motion where

$$f_n(s) = -\frac{1}{\nu_n}\frac{d}{ds}\left[\gamma(s) - g_n(s)\right] \tag{29}$$

and

$$g_n(s) = \gamma(s) - \frac{|\nu_n|}{2}\left\{\hat{\gamma}(|\nu_n|)\exp(-|\nu_n|s) + \int_0^\infty du\,\gamma(u)\exp\left[-|\nu_n(s-u)|\right]\right\} \tag{30}$$

are auxiliary functions introduced in (I31) and (I34).

B. Extremal imaginary time path for temperatures near T_c

With $\phi(\sigma)$ we have identified the direction in function space along which the minimal action path diverges for inverse temperatures near θ_c in the harmonic approximation. To determine the extremal imaginary time path near θ_c for an anharmonic potential, we make the ansatz

$$\bar{q}(\sigma) = \frac{1}{\theta}\sum_{l=1}^{\infty} Q_{2l}\,\sin(\nu_l\sigma) + \hat{Q}\,\phi(\sigma) + \hat{q}(\sigma). \tag{31}$$

Anharmonic terms will be seen to strongly affect the mode amplitude $\hat{Q}$. We recall that $\bar{q}'$ and $\bar{q}$ as well as the end points of the real time path $x(s)$ are assumed to be at most of order $\xi^{-1/4}$ or smaller. Then the mode amplitude $\hat{Q}$ may become at most of order $\xi^{-3/4}$. This assumption will be confirmed self-consistently below. Inserting (31) into the equation of motion (10) we gain, by use of (3),

$$u_l^{-1}\,Q_{2l} + 2\sum_{k=2}^{\infty} c_{2k}\xi^{2k-2}\int_0^\theta d\sigma\,\sin(\nu_l\sigma)\bar{q}(\sigma)^{2k-1} = -2\nu_l\bar{x} - 2f_l[x(s)], \qquad l = 1,2,3,\ldots \tag{32}$$

and

$$\Lambda\,\hat{Q} - \frac{1}{1+\theta\Lambda}\sum_{k=2}^{\infty} c_{2k}\xi^{2k-2}\int_0^\theta d\sigma\phi(\sigma)\bar{q}(\sigma)^{2k-1} = \bar{b}. \tag{33}$$

Equation (32) for the even Fourier mode amplitudes can be solved perturbatively by expanding about the harmonic path. We set

$$Q_{2l} = Q_{2l,0} + \xi^{1/2}\,Q_{2l,1} + O(\xi^{3/4}), \tag{34}$$

where the $Q_{2l,0}$ are of order $\xi^{-1/4}$ and describe the solution in the harmonic approximation. The $Q_{2l,1}$ are also of order $\xi^{-1/4}$ and take into account corrections due to anharmonic terms. Hence we obtain

$$Q_{2l,0} = -u_l\left\{2\nu_l\bar{x} + 2f_l[x(s)]\right\} \tag{35}$$

and

$$Q_{2l,1} = -3c_4\xi^{3/2}u_l\hat{Q}^2\sum_{m=1}^{\infty} D_{2,ml}\,Q_{2m,0}. \tag{36}$$

Here we have introduced the coefficients

$$D_n = \frac{2}{\theta}\int_0^\theta d\sigma\,\phi(\sigma)^n \tag{37}$$

and

$$D_{n,l_1\cdots l_k} = \frac{2}{\theta}\int_0^\theta d\sigma\,\phi(\sigma)^n\prod_{m=1}^{k}\sin(\nu_{l_m}\sigma). \tag{38}$$

Further, we have made use of the fact that $D_{3,l}$ vanishes.

For the marginal mode amplitude $\hat{Q}$ one has from (33), apart from corrections of order $\xi^{3/4}$,

$$\Lambda\,\hat{Q} - c_4\xi^2\frac{\theta}{2}D_4(1-\theta\Lambda)\hat{Q}^3 - 3c_4\xi^2\hat{Q}^2\int_0^\theta d\sigma\phi(\sigma)^3\hat{q}(\sigma) = \bar{b}. \tag{39}$$

Now, from (35) we recover the harmonic solution for the even Fourier mode amplitudes apart from corrections that are at most of order $\xi^{1/4}$. Further, in view of (14) the coefficient $\bar{b}$ is of order $\xi^{-1/4}$ or smaller. Hence, from (39) we see that for $\Lambda \to 0$ the coefficient $\hat{Q}$ no longer diverges but saturates at a finite value of order $\xi^{-3/4}$ or smaller, as assumed above. The purely harmonic solution fails and the anharmonic term becomes important when Λ is of order $\xi^{1/2}$ or smaller. We note that the third term and the term containing ΛQ^3 on the left-hand side of (39) give a correction of order $\xi^{1/4}$ while the second term may be of order $\xi^{-1/4}$.

To make the ξ dependence more explicit, it is advantageous to set

$$Q \equiv \frac{1}{2\theta}\,\xi^{1/2}\,\hat{Q}. \tag{40}$$

The amplitude Q is of order $\xi^{-1/4}$ or smaller near the caustic and thus of the same order of magnitude as the end points. Then, using (14) the cubic equation (39) takes the form

$$\frac{\Lambda}{\xi^{1/2}}\,Q - 2\theta^3 c_4\,D_4(1-\theta\Lambda)\,\xi^{1/2}Q^3 - 6\theta c_4\xi Q^2\int_0^\theta d\sigma\phi(\sigma)^3\times\hat{q}(\sigma) = \frac{1}{2\theta}\left[\bar{r} - \frac{i}{\theta}\sum_{n=-\infty}^{\infty} u_n\,g_n[x(s)]\right]. \tag{41}$$

The properties of this equation will be discussed in Sec. V D. The minimal action path in imaginary time (31) is given in terms of the solutions Q of (41) by virtue of (35), (36), and (40). Of course, (41) can be evaluated only when the real time path $x(s)$ is known.

IV. EXTREMAL REAL TIME PATHS

After the study of the extremal imaginary time path $\bar{q}(\sigma)$, we proceed and determine the extremal real time paths $r(s)$ and $x(s)$. Due to the coupling of $\bar{q}(\sigma)$ to the real time motion, the real time paths are also affected by anharmonicities of the potential field. The corresponding equations of motions can be solved perturbatively by expanding about the paths in the purely harmonic potential. This expansion proceeds in powers of $\xi^{1/2}$. In Sec. IV A we specify the equations of motions for $r(s)$ and $x(s)$, which will be solved in Secs. IV B–IV D.

A. Equations of motions

Let us first consider the equation of motion (I42) for the real time path $r(s)$

$$\ddot{r}+\frac{d}{ds}\int_0^s ds'\gamma(s-s')r(s')+\frac{1}{2}\frac{d}{dr}[V(r+x/2)+V(r-x/2)]=i\int_0^t ds'K'(s-s')x(s')+\int_0^\theta d\sigma K^*(s-i\sigma)\bar{q}(\sigma). \quad (42)$$

The inhomogeneity reads

$$i\int_0^t ds'K'(s-s')x(s')+\int_0^\theta d\sigma K^*(s-i\sigma)\bar{q}(\sigma)$$

$$=i\int_0^t ds'\,\tilde{R}(s,s')x(s')+\tilde{F}(s), \quad (43)$$

where we have inserted the result (31) for $\bar{q}(\sigma)$ and made use of (35) and (36) to obtain the right-hand side. Here

$$\tilde{R}(s,s')=R(s,s')+\xi^{1/2}\,\delta R(s,s') \quad (44)$$

with

$$R(s,s')=K'(s-s')+\frac{1}{\theta}\sum_{n=-\infty}^{\infty}u_n\,[g_n(s)g_n(s')-f_n(s)f_n(s')] \quad (45)$$

and

$$\delta R(s,s')=6c_4\xi^{1/2}\theta Q^2\sum_{n,n'=-\infty}^{\infty}D_{2,nn'}\,f_n(s)u_nf_{n'}(s)u_{n'}, \quad (46)$$

which are both of order 1 or smaller. Furthermore,

$$\tilde{F}(s)=F(s)+\xi\,\delta F(s), \quad (47)$$

where

$$F(s)=-i\bar{x}C_2(s)+2\theta\frac{Q}{\xi^{1/2}}C_1(s)-2\theta\gamma(s)\left(\frac{\Lambda Q}{\xi^{1/2}}-\frac{\bar{b}}{2\theta}\right) \quad (48)$$

and

$$\delta F(s)=6ic_4\theta Q^2\bar{x}\sum_{n,n'=-\infty}^{\infty}f_n(s)u_nu_{n'}\nu_{n'}D_{2,nn'} \quad (49)$$

are both of order $\xi^{-3/4}$ or smaller. In (48) we have introduced the functions [see also (I62)]

$$C_1(s)=\frac{1}{\theta}\sum_{n=-\infty}^{\infty}u_n\,g_n(s),$$

$$C_2(s)=\frac{1}{\theta}\sum_{n=-\infty}^{\infty}\nu_nu_n\,f_n(s). \quad (50)$$

For high enough temperatures, where the cubic and quadratic terms in (41) may be disregarded, one has

$$\tilde{R}(s,s')=R(s,s') \quad (51)$$

and

$$\tilde{F}(s)=F(s)=\frac{\bar{r}}{\Lambda}C_1(s)-i\bar{x}C_2(s)-\frac{i}{\Lambda}\int_0^t ds'\,C_1(s)C_1(s')x(s') \quad (52)$$

which is the known high-temperature result (I61). However, for temperatures close to T_c, the amplitude Q is of order $\xi^{-1/4}$ or smaller and $F(s)$ becomes of order $\xi^{-3/4}$ or smaller. For large enough times t we then have

$$\max_{0<s<t}r(s)=O(\xi^{-3/4}). \quad (53)$$

Thus anharmonic terms in (42) become of order $\xi^{-1/4}$ and cannot be neglected since they lead to terms of order $\xi^{-1/2}$ in the minimal effective action. We have

$$\frac{1}{2}\frac{d}{dr}[V(r+x/2)+V(r-x/2)]$$

$$=-r+c_4\xi^2r^3+O(\xi^{3/4}), \quad (54)$$

where we have assumed that $x(s)$ is of order $\xi^{-1/4}$ or smaller, which will be confirmed at the end of Sec. IV B. The equation of motion (42) can then be solved perturbatively using the ansatz

$$r(s)=r_0(s)+\xi^{1/2}r_1(s)+\xi r_2(s)+O(\xi^{3/4}), \quad (55)$$

where $r_0(s)$ may be of order $\xi^{-3/4}$ with $r_0(0)=r_i$ and $r_0(t)=r_f$, while $r_1(s)$ and $r_2(s)$ are also at most of order $\xi^{-3/4}$ with $r_1(0)=r_1(t)=0$ and $r_2(0)=r_2(t)=0$.

Now let us consider the minimal action path $x(s)$. Ac-

cording to (I43), the equation of motion for $x(s)$ reads

$$\ddot{x} - \frac{d}{ds}\int_s^t ds'\gamma(s'-s)x(s') + 2\frac{d}{dx}\left[V(r+x/2)+V(r-x/2)\right] = 0. \quad (56)$$

To solve (56) perturbatively we set

$$x(s) = x_0(s) + \xi^{1/2}x_1(s) + \xi x_2(s) + O(\xi^{5/4}). \quad (57)$$

The part $x_0(s)$ will be seen to be identical to the harmonic solution (I67), which is of order $\xi^{-1/4}$ and fulfills $x_0(0) = x_i$ and $x_0(t) = x_f$. The other parts $x_1(s)$ and $x_2(s)$ are also at most of order $\xi^{-1/4}$ with $x_1(0) = x_1(t) = 0$ and $x_2(0) = x_2(t) = 0$. According to (8) and (55) one has

$$2\frac{d}{dx}\left[V(r+x/2)+V(r-x/2)\right] = -x + 3c_4\xi^2 x r^2 + O(\xi^{5/4}). \quad (58)$$

We note that $x(s)$ must be evaluated up to corrections of order $\xi^{3/4}$ since this path is coupled to the imaginary time path $\bar{q}(\sigma)$ in the effective action (7).

B. Zeroth-order perturbation theory

In leading order in ξ one gains from (42)

$$\ddot{r}_0 + \frac{d}{ds}\int_0^s ds'\gamma(s-s')r_0(s') - r_0 = 2\theta\frac{Q}{\xi^{1/2}}C_1(s). \quad (59)$$

The solution for $r_0(s)$ is straightforward. We introduce the propagator $G_+(s)$ of the homogeneous equation with the initial conditions $G_+(0) = 0$ and $\dot{G}_+(0) = 1$ which has the Laplace transform

$$\hat{G}_+(z) = \left[z^2 + z\hat{\gamma}(z) - 1\right]^{-1}. \quad (60)$$

The solution of (59) is then obtained as

$$r_0(s) = r_f\frac{G_+(s)}{G_+(t)} + r_i\left[\dot{G}_+(s) - \frac{G_+(s)}{G_+(t)}\dot{G}_+(t)\right] + r_0^a(s), \quad (61)$$

where

$$r_0^a(s) = 2\theta\frac{Q}{\xi^{1/2}}G_+(s)\left[C_1^+(s) - C_1^+(t)\right]. \quad (62)$$

Here we have introduced the time-dependent functions

$$C_n^+(s) = \int_0^s ds'\frac{G_+(s-s')}{G_+(s)}C_n(s'),\ n = 1,2. \quad (63)$$

Clearly, the last term in (61) obeys $r_0^a(0) = r_0^a(t) = 0$ and depends, through the amplitude Q, on the anharmonicities of the potential. $r_0^a(s)$ becomes of order $\xi^{-3/4}$ or smaller near θ_c, while the first two terms in (61) always remain of order $\xi^{-1/4}$ and guarantee that $r(s)$ fulfills the boundary conditions $r(0) = r_i$ and $r(t) = r_f$.

Correspondingly, we obtain from (56)

$$\ddot{x}_0 - \frac{d}{ds}\int_s^t ds'\gamma(s'-s)x_0(s') - x_0 = 0. \quad (64)$$

This equation of motion for $x_0(s)$ is homogeneous and can be shown to be the backward equation of the equation of motion for $r_0(s)$ for vanishing inhomogeneity [6]. Hence the solution of (64) reads

$$x_0(s) = x_i\frac{G_+(t-s)}{G_+(t)} + x_f\left[\dot{G}_+(t-s) - \frac{G_+(t-s)}{G_+(t)}\dot{G}_+(t)\right]. \quad (65)$$

The result (65) confirms that for end points x_i,x_f of order $\xi^{-1/4}$ or smaller, $x(s)$ is at most of order $\xi^{-1/4}$, as assumed above.

C. First-order perturbation theory

To the next order in $\xi^{1/2}$ one obtains from (42) and (61)

$$\ddot{r}_1 + \frac{d}{ds}\int_0^s ds'\gamma(s-s')r_1(s') - r_1 + c_4\xi^{3/2}r_0^{a3} = i\xi^{-1/2}\int_0^t ds'\,R(s,s')x_0(s') - i\frac{\bar{x}C_2(s)}{\xi^{1/2}} - \frac{2\theta\gamma(s)}{\xi^{1/2}}\left(\frac{\Lambda Q}{\xi^{1/2}} - \frac{\bar{b}}{2\theta}\right). \quad (66)$$

With the propagator $G_+(s)$ introduced in (60), we find for the solution of (66)

$$\xi^{1/2}r_1(s) = \int_0^s ds'\,G_+(s-s')\left\{i\int_0^t ds''\,R(s',s'')x_0(s'') + \left[F(s') - 2\theta\frac{Q}{\xi^{1/2}}C_1(s')\right] - c_4\xi^2 r_0^a(s')^3\right\} - \frac{G_+(s)}{G_+(t)}\int_0^t ds'\,G_+(t-s')\left\{i\int_0^t ds''\,R(s',s'')x_0(s'') + \left[F(s') - 2\theta\frac{Q}{\xi^{1/2}}C_1(s')\right] - c_4\xi^2 r_0^a(s')^3\right\}. \quad (67)$$

On the other hand, according (58) and (61), the equation of motion for $x_1(s)$ is readily obtained from (56) as

$$\ddot{x}_1 - \frac{d}{ds}\int_s^t ds'\gamma(s'-s)x_1(s') - x_1 = -3c_4\xi^{3/2}x_0 r_0^{a2}. \tag{68}$$

Thus we get the solution

$$x_1(s) = -3c_4\xi^{3/2}\left[\int_s^t ds'\, G_+(s'-s)x_0(s')r_0^a(s')^2 - \frac{G_+(t-s)}{G_+(t)}\int_0^t ds'\, G_+(s')x_0(s')r_0^a(s')^2\right]. \tag{69}$$

This combines with (62) to yield, for $x_1(s)$ the compact form,

$$\xi^{1/2}x_1(s) = -12c_4\theta^2\,\xi\,Q^2\; G_+(t-s) \times\Big\{x_i\left[I_{i,0}(t,s) - I_{i,0}(t,0)\right] + x_f\left[I_{f,0}(t,s) - I_{f,0}(t,0)\right]\Big\}. \tag{70}$$

Here we have introduced the time-dependent functions

$$I_{\alpha,n}(t,s) = \frac{d^n}{ds^n}\int_s^t ds'\,\frac{G_+(s'-s)}{G_+(t-s)} \times G_+(s')^2\, G_\alpha(t,s')\left[C_1^+(s') - C_1^+(t)\right]^2 \tag{71}$$

with $\alpha = i, f$, where

$$G_i(t,s) = G_+(t-s)/G_+(t),$$
$$G_f(t,s) = \dot{G}_+(t-s) - G_+(t-s)\dot{G}(t)/G_+(t). \tag{72}$$

D. Second-order perturbation theory

Since the real time motion for $r(s)$ is directly coupled to the imaginary time path $\bar{q}(\sigma)$, the magnitude of $r(s)$ grows near T_c, as discussed in Sec. IV A. Hence second-order corrections to $r_0(s)$ must also be taken into account. From (42) and (61) we find

$$\ddot{r}_2 + \frac{d}{ds}\int_0^s ds'\gamma(s-s')r_2(s') - r_2 + 3c_4\xi r_0^{a2}\left(r_0 - r_0^a + \xi^{1/2}r_1\right) = i\xi^{-1/2}\int_0^t ds'\,\left[R(s,s')x_1(s') + \delta R(s,s')x_0(s')\right] + \delta F(s), \tag{73}$$

which yields

$$\xi r_2(s) = \int_0^s ds'\, G_+(s-s')\left\{i\xi^{1/2}\int_0^t ds''\,\left[R(s',s'')x_1(s'') + \delta R(s',s'')x_0(s'')\right] + \xi\delta F(s') - 3c_4\xi^2 r_0^a(s')^2\left[r_0(s') - r_0^a(s') + \xi^{1/2}r_1(s')\right]\right\} - \frac{G_+(s)}{G_+(t)}\int_0^t ds'\, G_+(t-s')\left\{i\xi^{1/2}\int_0^t ds''\,\left[R(s',s'')x_1(s'') + \delta R(s',s'')x_0(s'')\right] + \xi\delta F(s') - 3c_4\xi^2 r_0^a(s')^2\left[r_0(s') - r_0^a(s') + \xi^{1/2}r_1(s')\right]\right\}. \tag{74}$$

Now, with (61), (67), and (74) the extremal real time path $r(s)$ is evaluated up to corrections at most of order $\xi^{3/4}$ for end points r_i and r_f, which are at most of order $\xi^{-1/4}$.

The term in the effective action (7) that couples the real time and the imaginary time motion contains the path $x(s)$. Hence this path must be evaluated up to corrections of order $\xi^{3/4}$. From (58) and (61) we obtain

$$\ddot{x}_2 - \frac{d}{ds}\int_s^t ds'\gamma(s'-s)x_2(s') - x_2 = -3c_4\xi r_0^a\left\{2x_0\left[\xi^{1/2}r_1 + r_0 - r_0^a\right] + \xi^{1/2}x_1 r_0^a\right\}. \tag{75}$$

Thus we gain

$$\xi x_2(s) = -3c_4\xi^2\left\{\int_s^t ds'\, G_+(s'-s)r_0^a(s')\{2x_0(s')\left[\xi^{1/2}r_1(s') + r_0(s') - r_0^a(s')\right] + \xi^{1/2}x_1(s')r_0^a(s')\} - \frac{G_+(t-s)}{G_+(t)}\int_0^t ds'\, G_+(s')r_0^a(s')\{2x_0(s')\left[\xi^{1/2}r_1(s') + r_0(s') - r_0^a(s')\right] + \xi^{1/2}x_1(s')r_0^a(s')\}\right\}. \tag{76}$$

With (65), (70), and (76) the real time path $x(s)$ is determined apart from corrections that are at most of order $\xi^{5/4}$ for end points x_i and x_f of order $\xi^{-1/4}$. This suffices to perform a semiclassical approximation of the propagating function, as will be seen below.

Finally, let us discuss whether the above solutions for the real time paths are sufficient to determine the semiclassical approximation of the propagating function when the time interval t becomes large. The above trajectories connect end points within the barrier region of the nonlinear potential (8) by paths with turning points near the top of the potential barrier. Hence these trajectories remain also within the barrier region for all times. As mentioned above, we assume that the potential (8) becomes broader than its harmonic approximation for lower energies, where typically it passes into a well region. Clearly, in this case, for very long times end points within the barrier region may also be connected by trajectories moving back and forth through the well region. The corresponding contributions become in particular relevant for weak damping and long times. We will show at the end of Sec. VI that this leads to an upper bound of time for the validity of the semiclassical approximation of the propagating function based on the real time paths determined above.

V. MINIMAL EFFECTIVE ACTION

Having evaluated the minimal action paths, we may determine the density matrix in the semiclassical approximation by expanding the functional integral about the minimal action paths. In this section we first calculate the minimal effective action. The contribution of the fluctuations about the minimal action paths is evaluated in Sec. VI.

Using the equations of motions (10), (42), and (56), the minimal effective action (I28) in an anharmonic potential field may be written as

$$\Sigma(x_f, r_f, t, x_i, r_i, \bar{x}, \bar{r}) = \Sigma^h(x_f, r_f, t, x_i, r_i, \bar{x}, \bar{r}) + \Sigma^a(x_f, r_f, t, x_i, r_i, \bar{x}, \bar{r}), \tag{77}$$

where $\Sigma^h(x_f, r_f, t, x_i, r_i, \bar{x}, \bar{r})$ denotes the harmonic result (I68) and

$$\begin{aligned}\Sigma^a(x_f, r_f, t, x_i, r_i, \bar{x}, \bar{r}) = {} & \frac{i}{2}\left[\bar{q}\,\dot{\bar{q}}^a(\theta) - \bar{q}'\,\dot{\bar{q}}^a(0)\right] + i\int_0^\theta d\sigma\left[V(\bar{q}) - \frac{\bar{q}}{2}\frac{dV(\bar{q})}{d\bar{q}}\right] \\ & -\frac{1}{2}\int_0^\theta d\sigma\int_0^t ds\, K^*(s-i\sigma)\bar{q}^a(\sigma)x^h(s) - \frac{1}{2}\int_0^\theta d\sigma\int_0^t ds\, K^*(s-i\sigma)\bar{q}(\sigma)x^a(s) \\ & + x_f\,\dot{r}^a(t) - x_i\,\dot{r}^a(0) - \frac{i}{2}\int_0^t ds\int_0^t du\, K'(s-u)\left[2x^a(s)x^h(u) + x^a(s)x^a(u)\right] \\ & + \int_0^t ds\left\{x(s)\frac{1}{2}\frac{d}{dr}\left[V\left(r+\frac{x}{2}\right) + V\left(r-\frac{x}{2}\right)\right] - V\left(r+\frac{x}{2}\right) + V\left(r-\frac{x}{2}\right)\right\}. \end{aligned} \tag{78}$$

Here we have split the minimal action paths into the harmonic solution and an anharmonic part according to

$$\begin{aligned} x(s) &= x^h(s) + x^a(s), \\ \bar{q}(\sigma) &= \bar{q}^h(\sigma) + \bar{q}^a(\sigma), \\ r(s) &= r^h(s) + r^a(s). \end{aligned} \tag{79}$$

The harmonic parts are $x^h(s) = x_0(s)$ given by (65) as well as $\bar{q}^h(\sigma)$ and $r^h(s)$ specified in (I57) and (I66), respectively.

Using the minimal action paths calculated perturbatively in Sec. IV, one obtains from (57)

$$x^a(s) = \xi^{1/2}\,x_1(s) + \xi x_2(s) + O(\xi^{5/4}) \tag{80}$$

and from (31) and (36)

$$\bar{q}^a(\sigma) = \left(\frac{2\theta Q}{\xi^{1/2}} - \frac{\bar{b}}{\Lambda}\right)\phi(\sigma) + \xi^{1/2}\,\frac{1}{\theta}\sum_{l=1}^{\infty} Q_{2l,1}\sin(\nu_l\sigma) + O(\xi^{3/4}). \tag{81}$$

Finally, (25) and (55) yield

$$\begin{aligned} r^a(s) = {} & r_0^a(s) + \xi\, r_2(s) - G_+(s)\left[C_1^+(s) - C_1^+(t)\right]\frac{\bar{b}}{\Lambda} \\ & - G_+(s)\left\{\left(\frac{2\theta\Lambda Q}{\xi^{1/2}} - \bar{b}\right)\left[\gamma_i(s) - \gamma_i(t)\right] \right. \\ & \left. + 8c_4\theta^3\,\xi^{1/2}\,Q^3\,\left[j_i(s) - j_i(t)\right]\right\} + O(\xi^{3/4}). \end{aligned} \tag{82}$$

Here we have introduced the time-dependent functions

$$\gamma_\alpha(s) = \int_0^s ds'\,\gamma(s')\,G_\alpha(s,s') \tag{83}$$

and

$$j_\alpha(s) = \int_0^s ds'\,G_\alpha(s,s')\,G_+(s')^3\,\left[C_1^+(s') - C_1^+(t)\right]^3, \tag{84}$$

where $\alpha = i, f$. We note that near T_c the harmonic part Σ^h as well as the anharmonic correction Σ^a in (77) diverge; however, the divergencies cancel and the full minimal effective action remains finite.

Now inserting (81) and (82) as well as $x(s)$ as given by (57) into the anharmonic part (78) of the effective action and adding the harmonic part (I68), the minimal effective action may be written as

$$\Sigma(x_f,r_f,t,x_i,r_i,\bar{x},\bar{r})$$

$$=\sum_{k=0}^{2}\xi^{k/2}\left[\Sigma_\theta^k(\bar{x},\bar{r})+\Sigma_t^k(x_f,r_f,t,x_i,r_i,\bar{x},\bar{r})\right]+O(\xi^{1/2}). \tag{85}$$

Here the functions Σ_θ^k are at most of order ξ^{-1} and contain those contributions to Σ that are nonvanishing for $x(s)=r(s)=0$. The remaining parts Σ_t^k are also of order ξ^{-1} or smaller. These functions will be evaluated in the following sections. Afterward, in Sec. V D, the behavoir of the marginal mode amplitude Q is discussed.

A. Minimal effective action in leading order

With the imaginary time path (81) one gains from (78)

$$\Sigma_\theta^0(\bar{x},\bar{r})=i\left(\theta\frac{Q\bar{r}}{\xi^{1/2}}-2c_4\theta^5D_4Q^4\right), \tag{86}$$

which is the dominant term of the imaginary time action of order $1/\xi$ for inverse temperatures below and near θ_c. Obviously, the action is independent of $\bar{x}$ and essentially determined by the amplitude Q of the marginal mode that remains finite near T_c.

Since the time dependence of the minimal action paths in real time is determined essentially by the dynamics at a parabolic barrier, it is advantageous to use the functions

$$A(t)=-\frac{1}{2}\,\Theta(t)\,G_+(t) \tag{87}$$

and

$$S(t)=\Lambda\dot{G}_+(t)+G_+(t)\,C_1^+(t), \tag{88}$$

where $\Theta(t)$ denotes the step function and $C_1^+(t)$ is given in (63). In terms of these functions $\Sigma_t^k(x_f,r_f,t,x_i,r_i,\bar{x},\bar{r})$ can be expressed conveniently. To leading order one finds from (81) and (65)

$$\Sigma_t^0(x_f,r_f,t,x_i,r_i,\bar{x},\bar{r})$$

$$=\frac{\theta Q}{\xi^{1/2}}\,x_f\left[\dot{S}(t)-S(t)\frac{\dot{A}(t)}{A(t)}\right]-\frac{\theta Q}{\xi^{1/2}}\,x_i\,\frac{S(t)}{2A(t)}. \tag{89}$$

Clearly, according to (86) and (89) the leading-order terms in the minimal effective action are of order ξ^{-1} and therefore much larger than the action in the purely harmonic case, which is of order $\xi^{-1/2}$ for coordinates that are of order $\xi^{-1/4}$.

B. First-order contributions

Next-order terms in the expansion (85) lead to contributions to the minimal effective action that are of order $\xi^{-1/2}$ or smaller. Correspondingly, one obtains from (31) and (78)

$$\xi^{1/2}\Sigma_\theta^1(\bar{x},\bar{r})=i\left[\frac{\Omega}{2}\bar{x}^2-c_4\theta^4\left(4D_3\,\xi^{1/2}\bar{r}Q^3+\frac{32c_6}{3c_4}\,\theta^3D_6\,\xi Q^6\right)\right], \tag{90}$$

where Ω is defined in (I70). Note that the $\bar{x}^2$-dependent term appears already in the imaginary time action of the purely harmonic potential. For high enough temperatures and $x(s)\equiv 0$, the two actions in (86) and (90) sum to yield

$$S_\theta(\bar{x},\bar{r})=\Sigma_\theta^0(\bar{x},\bar{r})+\xi^{1/2}\Sigma_\theta^1(\bar{x},\bar{r})\Big|_{x(s)=0}=i\frac{\bar{r}^2}{2\Lambda}+i\frac{\Omega}{2}\,\bar{x}^2, \tag{91}$$

which is the known minimal imaginary time action of a damped inverted harmonic oscillator (I69).

Using the real time part Σ_t^h of the harmonic minimal effective action (I74) as well as (62), (65), and (81), one gets, for the real time part of the action in an anharmonic potential field in first order, the contribution

$$\xi^{1/2}\Sigma_t^1(x_f,r_f,t,x_i,r_i,\bar{x},\bar{r})$$

$$\begin{aligned}
&=\Sigma_t^h(x_f,r_f,t,x_i,r_i,\bar{x},\bar{r})+x_f\left(\frac{\theta\Lambda}{\xi^{1/2}}\,Q-\bar{r}\right)\left[2\ddot{A}(t)-\frac{2\dot{A}(t)^2}{A(t)}\right]-x_f\bar{r}\left[\frac{\dot{S}(t)}{\Lambda}-\frac{S(t)}{\Lambda}\frac{\dot{A}(t)}{A(t)}\right]\\
&-x_i\left(\frac{\theta\Lambda}{\xi^{1/2}}\,Q-\bar{r}\right)\frac{\dot{A}(t)}{A(t)}+x_i\bar{r}\frac{S(t)}{2\Lambda A(t)}+\frac{i}{2}x_i^2\frac{[S(t)+2\Lambda\dot{A}(t)]^2}{4A(t)^2\Lambda}\\
&+ix_ix_f\frac{S(t)+2\Lambda\dot{A}(t)}{2A(t)\Lambda}\left\{\frac{\dot{A}(t)}{A(t)}\left[S(t)+2\Lambda\dot{A}(t)\right]-\dot{S}(t)-2\Lambda\ddot{A}(t)\right\}\\
&+\frac{i}{2}x_f^2\frac{1}{\Lambda}\left[\dot{S}(t)-\frac{\dot{A}(t)}{A(t)}S(t)+2\Lambda\ddot{A}(t)-2\Lambda\frac{\dot{A}(t)^2}{A(t)}\right]^2\\
&-4c_4\xi^{1/2}\theta^3Q^3x_f\left\{\theta D_4\gamma_f(t)+6A(t)C_{f,1}(t)-3I_{f,0}(t,0)\left[S(t)+2\Lambda\dot{A}(t)\right]+2j_f(t)-F_3^f(t)\right\}\\
&-4c_4\xi^{1/2}\theta^3Q^3x_i\left\{\theta D_4\gamma_i(t)+6A(t)C_{i,1}(t)-3I_{i,0}(t,0)\left[S(t)+2\Lambda\dot{A}(t)\right]+2j_i(t)-F_3^i(t)\right\}.
\end{aligned} \tag{92}$$

Here the influence of the anharmonicities on the real time part of the effective action is described by the time-dependent functions $\gamma_\alpha(t)$ and $j_\alpha(t)$ specified in (83) and (84) as well as

$$C_{\alpha,n}(t) = \int_0^t ds\, C_n(s)\, \frac{G_+(t-s)}{G_+(t)}\, I_{\alpha,0}(t,s) = \int_0^t ds \frac{G_+(s)^3}{G_+(t)} G_\alpha(t,s)\, \left[C_1^+(s) - C_1^+(t)\right]^2 C_n^+(s), \tag{93}$$

where $C_n^+(s)$ is given in (63) and $\alpha = i, f$.

Using the Laplace transform of the propagator (60) one gains from (83)

$$\gamma_i(t) = \int_0^t ds\, \frac{G_+(s)}{G_+(t)} - \frac{2\dot{A}(t)+1}{2A(t)} \tag{94}$$

and

$$\gamma_f(t) = 2\ddot{A}(t) - 2A(t) - \frac{\dot{A}(t)+2\dot{A}(t)^2}{A(t)} + 2\dot{A}(t)\int_0^t ds\, \frac{G_+(s)}{G_+(t)}. \tag{95}$$

Furthermore, the functions

$$F_p^{\alpha_1\cdots\alpha_m}(t) = \frac{2}{\theta}\int_0^\theta d\sigma\, \phi(\sigma)^p \times \prod_{k=1}^m \left\{ \sum_{n=-\infty}^{\infty} u_n \left[\cos(\nu_n\sigma) - 1\right] \times \int_0^t ds\, g_n(s) G_{\alpha_k}(t,s)\right\} \tag{96}$$

take into account couplings between the anharmonic corrections of the imaginary and the real time minimal action paths. We note that the divergent terms for $\Lambda \to 0$ in Σ_t^h cancel against terms explicitly given in (92) so that $\xi^{1/2}\Sigma_t^1$ remains finite at T_c.

C. Second-order contributions

The second-order contributions to the minimal effective action (85) are at most of order 1. For the imaginary time part we gain with (31)

$$\xi\Sigma_\theta^2(\bar{x},\bar{r}) = -ic_4\theta^4\left(\frac{3}{\theta}D_2\,\xi\bar{r}^2Q^2 + \frac{32c_6}{c_4}\theta^2 D_5\,\xi^{3/2}\bar{r}Q^5\right). \tag{97}$$

Using (80)–(82) one obtains, from (78) for the real time contribution after a tedious but straightforward calculation

$$\xi\Sigma_t^2(x_f,r_f,t,x_i,r_i,\bar{x},\bar{r}) = +6ic_4\theta^2\,\xi\,Q^2\,\sigma_t(x_f,r_f,t,x_i,r_i,\bar{x},\bar{r}), \tag{98}$$

where σ_t is of order $\xi^{-1/2}$ or smaller and given by

$$\begin{aligned}
\sigma_t(x_f,r_f,t,x_i,r_i,\bar{x},\bar{r}) &= x_i x_f\left\{[S(t)+2\Lambda\dot{A}(t)][\gamma_f(t)I_{i,0}(t,0)+\gamma_i(t)I_{f,0}(t,0)] + 2A(t)[\gamma_f(t)C_{i,1}(t)+\gamma_i(t)C_{f,1}(t)] + \frac{F_2^{if}(t)}{\theta}\right\}\\
&+x_i^2\left\{[S(t)+2\Lambda\dot{A}(t)]\gamma_i(t)I_{i,0}(t,0) + 2A(t)\gamma_i(t)C_{i,1}(t) + \frac{F_2^{ii}(t)}{2\theta}\right\}\\
&+x_f^2\left\{[S(t)+2\Lambda\dot{A}(t)]\gamma_f(t)I_{f,0}(t,0) + 2A(t)\gamma_f(t)C_{f,1}(t) + \frac{F_2^{ff}(t)}{2\theta}\right\} - i\bar{r}x_iF_2^i(t) - i\bar{r}x_fF_2^f(t)\\
&-24ic_4\xi^{1/2}\theta^3Q^3x_i\left\{\theta D_4A(t)[\gamma_{i,i}(t)-\gamma_iI_{i,0}(t,0)] - j_i^+(t) - 2A(t)j_i(t)I_{i,0}(t,0) + \frac{2c_6}{9c_4^2}F_5^i(t)\right\}\\
&-24ic_4\xi^{1/2}\theta^3Q^3x_f\left\{\theta D_4A(t)[\gamma_{i,f}(t)-\gamma_iI_{f,0}(t,0)] - j_f^+(t) - 2A(t)j_i(t)I_{f,0}(t,0) + \frac{2c_6}{9c_4^2}F_5^f(t)\right\}.
\end{aligned} \tag{99}$$

Here the time-dependent functions $j_\alpha^+(t)$ and $\gamma_{\alpha,\beta}(t)$ contain the harmonic propagator $A(t)$ as well as $S(t)$ in higher than quadratic powers. They are defined by

$$j_\alpha^+(t) = \int_0^t ds\, j_i(s)\, G_\alpha(t,s)\, G_+(s)^3\, \left[C_1^+(s) - C_1^+(t)\right]^2 \tag{100}$$

and

$$\gamma_{\alpha,\beta}(t) = \int_0^t ds\, \gamma(s)\, G_\alpha(t,s)\, I_{\beta,0}(t,s), \tag{101}$$

where $I_{\beta,0}(t,s)$ is given by (71) with $\alpha,\beta = i,f$. Also, we have made use of the fact that the $C_n^+(t)$ can be expressed as [6]

$$C_1^+(t) = -\frac{S(t)+2\Lambda\dot{A}(t)}{2A(t)}, \quad C_2^+(t) = -\frac{\dot{S}(t)}{2A(t)} + \Omega, \tag{102}$$

where according to (I70)

$$\Omega = \frac{1}{\theta}\sum_{n=-\infty}^{\infty} u_n\,[|\nu_n|\hat{\gamma}(|\nu_n|) - 1]. \tag{103}$$

D. Amplitude of the marginal mode

With the help of the above results we may write Eq. (41) for the amplitude Q in explicit form. By use of the solution (65) and (70) for the real time path $x(s)$ and (87) and (88), we gain

$$\frac{\Lambda}{\xi^{1/2}}\,Q - 2\theta^3 c_4\, D_4(1-\theta\Lambda)\,\xi^{1/2}Q^3 - 12\theta c_4 \xi Q^2\Bigg\{ix_i A(t)\left[\frac{F_3^i(t)}{4A(t)} + C_{i,1}(t) - I_{i,0}(t,0)C_1^+(t)\right]$$

$$+ix_f A(t)\left[\frac{F_3^f(t)}{4A(t)} + C_{f,1}(t) - I_{f,0}(t,0)C_1^+(t)\right] + \frac{\theta}{4}D_3\,\bar{r}\Bigg\} = \frac{1}{2\theta}\left[\bar{r} - i\,x_i\,C_1^+(t) - i\,x_f\,2A(t)\dot{C}_1^+(t)\right]. \tag{104}$$

For $x(s) \equiv 0$ this result reduces to a cubic equation for $Q = Q(\bar{r})$. This latter equation has only one stable real solution for $\theta < \theta_c$ while for $\theta > \tilde{\theta}_c$, where $\tilde{\theta}_c \geq \theta_c$ depends on the particular value of $\bar{r}$, three real solutions exist, two of which are stable and one is unstable. For a detailed discussion for the case of vanishing damping, see [10]. On the other hand, for $x(s) \neq 0$ the inhomongeneity in (104) is complex. Then three, in general, complex solutions of (104) exist for all temperatures (see Fig. 1). One of these, denoted by Q_{se}, has for $\theta \ll \theta_c$ imaginary and real parts at most of order $\xi^{1/4}$ for end points $\bar{r}, x_i, x_f$ of order $\xi^{-1/4}$ and coincides with the high-temperature solution given in I. When the temperature is lowered the real part of this solution increases, while the imaginary part remains small (Fig. 1). Regarding physically relevant real fluctuations of the trajectories, this solution with amplitude Q_{se} is found to be stable also at low temperatures (see Sec. VI B). The two other solutions, with amplitudes denoted by Q_{sn} and Q_u, have large imaginary parts of opposite sign and small real parts for $\theta \ll \theta_c$ (Fig. 1). These solutions are unstable for $\theta < \theta_c$. As the temperature is lowered the imaginary parts of both solutions decrease. The real part of Q_{sn} increases and the Q_{sn} branch becomes stable below the critical temperature, while the real part of Q_u decreases and the Q_u branch remains unstable. The imaginary time path (31) near θ_c is completely determined by (35) and (36) and the solutions of the cubic equation (104).

As mentioned above, for high temperatures the cubic and quadratic terms in Eq. (104) can be neglected and the amplitude Q becomes a linear function of the coordinates $\bar{r}$, x_i, and x_f. Then the term in Σ_θ^0 containing $Q\bar{r}$ gives an $\bar{r}^2$ term, which leads with the term $i\Omega\bar{x}^2/2$

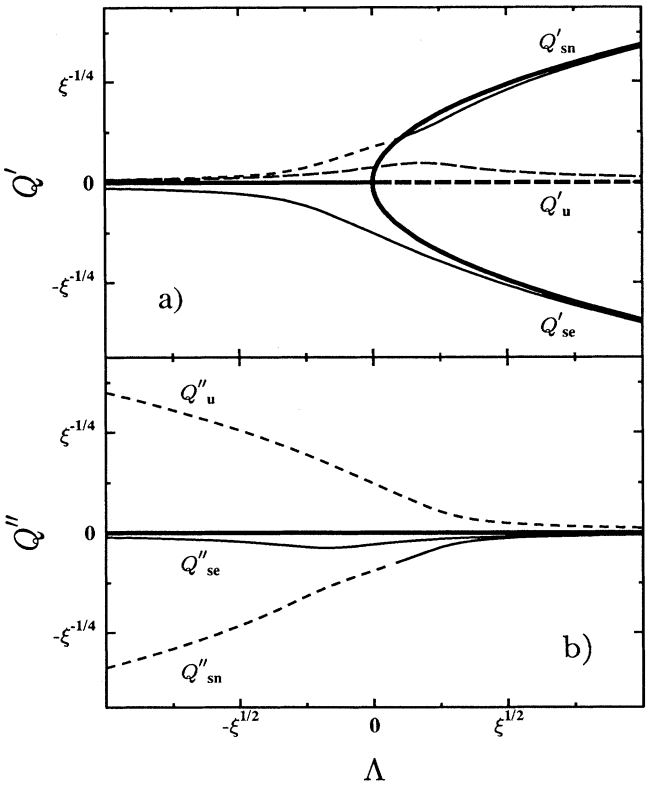

FIG. 1. (a) Real part Q' and (b) imaginary part Q'' of the marginal mode amplitude Q for $\bar{r} = x_i = x_f = 0$ (thick lines) and for $\bar{r} = x_i = x_f \neq 0$ (thin lines) versus the bifurcation parameter Λ. The solid lines represent stable branches and the dashed lines unstable branches.

in $\xi^{1/2}\Sigma_\theta^1$ to the imaginary time action (91) and time-dependent $\bar{r}x_i$ and $\bar{r}x_f$ terms. The remaining terms in $\xi^{1/2}\Sigma_\theta^1$ and the contribution $\xi\Sigma_\theta^2$ become at most of order ξ. The term $\xi\Sigma_t^2$ and the Q^3 terms in $\xi^{1/2}\Sigma_t^1$ are also of order ξ or smaller while the contributions in $\xi^{1/2}\Sigma_t^1$ and in Σ_t^0 containing Q give $\bar{r}x_i$ and $\bar{r}x_f$ terms as well as x_i^2, x_ix_f, and x_f^2 terms. Collecting the corresponding contributions, one recovers the known high-temperature result Σ_t^h in (I74).

VI. SEMICLASSICAL DENSITY MATRIX

With the minimal action (85) we have found the leading-order term of the path integral for the propagating function (6). The path integral now reduces to integrals over periodic paths $\eta(0) = \eta(t) = 0$ and $\eta'(0) = \eta'(t) = 0$ in real time and $y(0) = y(\theta) = 0$ in imaginary time describing the quantum fluctuations about the minimal action paths. As mentioned above, the relevant fluctuations give a contribution to the full effective action of order 1. Therefore, the semiclassical expansion is consistent only if the minimal effective action is also determined at least to order 1. In the expansion (85) we have neglected contributions to the minimal effective action of order $\xi^{1/2}$. As a consequence, we may determine the semiclassical propagating function (6) in the vicinity of the barrier top provided $\xi^{1/2}\xi^2/\epsilon^2 \ll 1$, i.e.,

$$\xi \ll \epsilon^{4/5}, \tag{105}$$

where ϵ is the semiclassical expansion parameter defined in (5), which is formally of order $\sqrt{\hbar}$. When condition (105) is not satisfied a semiclassical expansion is of course still feasible, but one has to go beyond the approximate results derived in the previous sections, eventually by use of numerical methods.

Now we proceed to determine the density matrix by expanding the effective action about the minimal action paths. This will be done in Sec. VI A. It will be seen that near T_c we have to go beyond a simple Gaussian approximation for the path integral over fluctuations about the imaginary time path. The corresponding non-quadratic fluctuation potential is discussed in Sec. VI B, leading to the time-dependent semiclassical density matrix. In particular, in Sec. VI C we consider the $t \to 0$ limit and gain an expression for the equilibrium density matrix near T_c.

A. Quantum fluctuations and fluctuation potential

Since the deviations $\eta(s)$, $\eta'(s)$, and $y(\sigma)$ from the minimal action paths in real and imaginary time describe quantum fluctuations, it is natural to scale them with the quantum length scale $q_0 = \sqrt{\hbar/2M\omega_0}$. In view of (5) and the dimensionless formulation we then have, for an arbitrary real time path,

$$q(s) = q_{\rm ma}(s) + (\epsilon/\xi)\,\eta(s), \tag{106}$$

where $q_{\rm ma}(s)$ denotes the minimal action path in real time. Correspondingly, for the imaginary time path

$$\bar{q}(\sigma) = \bar{q}_{\rm ma}(\sigma) + (\epsilon/\xi)\,y(\sigma). \tag{107}$$

First, let us consider the real time fluctuations. In the corresponding second-order variational operator the anharmonicities of the barrier potential are at most of order $\xi^{1/2}$ and can therefore be neglected. As in I, the contribution of the Gaussian fluctuations around each of the two real time paths $q(s)$ and $q'(s)$ gives

$$\int\mathcal{D}[\eta]\ \exp\left\{\frac{i}{4}\int_0^t ds\,\eta(s)\left[\ddot{\eta}(s) + \int_0^s du\,\gamma(s-u)\,\dot{\eta}(u) - \eta(s)\right]\right\} = \frac{1}{\sqrt{8\pi|A(t)|}}. \tag{108}$$

Note that, according to (I22), the real time paths $q(s)$ and $q'(s)$ are related to the sum and difference paths considered in the previous sections by $r(s) = [q(s) + q'(s)]/2$ and $x(s) = q(s) - q'(s)$.

A corresponding Gaussian approximation for the fluctuations about the imaginary time path gives (I78)

$$\int\mathcal{D}[y]\ \exp\left\{-\frac{1}{4}\int_0^\theta d\sigma y(\sigma)\left[-\ddot{y}(\sigma) + \int_0^\theta d\sigma'\,k(\sigma-\sigma')\,y(\sigma') - y(\sigma)\right]\right\} = \frac{1}{\sqrt{-\Lambda}}\,\frac{1}{\sqrt{4\pi\theta^2}}\prod_{n=1}^{\infty}\nu_n^2\,u_n. \tag{109}$$

However, when the inverse temperature is increased, this simple semiclassical approximation diverges for inverse temperatures near θ_c ($\Lambda \to 0$). This is due to the fact that the ϕ direction in function space becomes unstable, as discussed in Sec. III A. Then higher-order contributions in the expansion of the imaginary time action about the minimal action path have to be taken into account according to

$$\Sigma[0,0,\bar{q}] = \Sigma[0,0,\bar{q}_{\rm ma}] + \frac{1}{2}(\epsilon/\xi)^2\int_0^\theta d\sigma_1\int_0^\theta d\sigma_2\,\frac{\delta^2\Sigma[0,0,\bar{q}]}{\delta\bar{q}^2}\bigg|_{\bar{q}=\bar{q}_{\rm ma}} y(\sigma_1)\,y(\sigma_2) + \sum_{n=3}^{\infty}\frac{1}{n!}(\epsilon/\xi)^n\int_0^\theta d\sigma_1\cdots\int_0^\theta d\sigma_n\,\frac{d^nV(\bar{q})}{d\bar{q}^n}\bigg|_{\bar{q}=\bar{q}_{\rm ma}} y(\sigma_1)\cdots y(\sigma_n). \tag{110}$$

Here an arbitrary imaginary time path $\bar{q}(\sigma)$ is decomposed according to (107) and $\Sigma[0,0,\bar{q}]$ is the imaginary time part of the effective action (I28).

For the undamped case the breakdown of the Gaussian approximation near T_c has been investigated in detail previously [10]. We have shown that the amplitude of the minimal action path Q, which becomes marginal near θ_c, is associated with a marginal fluctuation mode amplitude Y_1. Hence one eigenvalue of the second-order variational operator vanishes at $\theta = \theta_c$ for the purely harmonic potential. As a consequence, the amplitude Y_1 becomes arbitrarily large while all other mode amplitudes remain of order 1. In a weakly anharmonic potential the harmonic fluctuation potential for the amplitude Y_1 is replaced by a stable, quartic fluctuation potential. This extends to the case of finite damping, where in the harmonic approximation $\phi(\sigma)$ is an eigenfunction of the second-order variational operator with an eigenvalue proportional to Λ. We note that $\phi(\sigma)$ satisfies the boundary conditions $\phi(0) = \phi(\theta) = 0$ required for fluctuations $y(\sigma)$. As a consequence, $\phi(\sigma)$ is the direction in function space corresponding to the marginal fluctuation mode. Now decomposing a fluctuation $y(\sigma)$ into a component $Y_1\phi(\sigma)$ and stable mode amplitudes and assuming that Y_1 becomes at most of order $\epsilon^{-1/2}$ while the other mode amplitudes remain of order 1, we obtain from (110) the nonquadratic fluctuation potential

$$\begin{aligned} V(Q,Y_1) &\equiv (\xi/\epsilon)^2 \left(\Sigma[0,0,\bar{q}] - \Sigma[0,0,\bar{q}_{\rm ma}]\right)|_{y(\sigma)=Y_1\phi(\sigma)} \\ &= \frac{1}{4}\Big[\left(-\Lambda + 6\theta^3 c_4 D_4\, \xi\, Q^2\right) Y_1^2 \\ &\quad + 2\theta^2 c_4 D_4\, \epsilon\, \xi^{1/2}\, Q\, Y_1^3 \\ &\quad + \frac{\theta}{4} c_4 D_4\, \epsilon^2\, Y_1^4\Big] + o(1). \end{aligned} \tag{111}$$

Accordingly, the divergent factor $1/\sqrt{-\Lambda}$ in (109) is replaced by the fluctuation integral

$$K(Q) = \frac{1}{\sqrt{4\pi}} \int_{-\infty}^{\infty} dY_1 \, \exp\left[-V(Q,Y_1)\right], \tag{112}$$

which remains finite for $\theta = \theta_c$. Here Q is determined by the cubic equation (104). From (111) one sees that the coefficient

$$\Lambda_1(Q) = -\Lambda + 6\theta^3 c_4 D_4 \xi Q^2 \tag{113}$$

of the harmonic term may vanish, but the remaining terms of the fluctuation potential always constrain Y_1 to fluctuation amplitudes at most of order $\epsilon^{-1/2}$. The region in parameter space of coordinates and temperature, where the full fluctuation potential (111) is needed, is investigated in the next section.

B. Evaluation of the fluctuation potential and semiclassical density matrix

Since the fluctuation potential depends on the solutions Q of the cubic equation (104), we first have to investigate the stability of the various branches of the mode amplitude Q. Then the behavior of the fluctuation potential $V(Q,Y_1)$ is discussed as a function of temperature and coordinates. From there we obtain the semiclassical density matrix in the region near T_c.

In the dynamical case, i.e., $x(s) \neq 0$, the amplitude Q determined by (104) is a complex time-dependent function of the coordinates $\bar{r}$, x_i, and x_f with three different branches, as discussed in Sec. V D, and $V(Q,Y_1)$ is defined in the complex Y_1 plane. However, since only real paths are of physical relevance, we consider fluctuations parallel to the real Y_1 axis only. For high temperatures these fluctuations about the Q_{se} branch of the cubic equation (104) have an eigenvalue $\Lambda_1(Q_{se}) \approx -\Lambda > 0$. With increasing inverse temperature the real part of Q_{se} also increases [see Fig. 1(a)] and anharmonic terms in $V(Q_{se},Y_1)$ become important for T near T_c. For temperatures sufficiently below T_c one has $\Lambda_1(Q_{se}) \approx 2\Lambda > 0$ and a simple semiclassical approximation of $K(Q_{se})$ is again appropriate. This shows that the minimal action path with amplitude Q_{se} is stable with respect to real fluctuations for high as well as for low temperatures. The two other solutions Q_{sn} and Q_u of (104) have large imaginary parts for high temperatures [see Fig. 1(b)]. As a consequence, one can show that $\mathrm{Re}\{\Lambda_1(Q_{sn})\}$ and $\mathrm{Re}\{\Lambda_1(Q_u)\}$ are negative and both branches are unstable. When the temperature is lowered the imaginary parts of these branches decrease. The real part of Q_{sn} increases as T_c is approached and becomes of order of the real part of Q_{se}, however, with an opposite sign [Fig. 1(a)]. Hence the corresponding minimal action path becomes stable for T near T_c. The real part of Q_u remains small so that for $T < T_c$ the eigenvalue $\Lambda_1(Q_u) \approx -\Lambda$ is negative and the corresponding minimal action path unstable.

Now let us consider the fluctuation potential $V(Q,Y_1)$. For real Q the potential (111) as a function of temperature has been investigated previously [10]. For complex Q, the above analysis shows that for high enough temperatures one has one stable minimal action path with amplitude Q_{se}, while for temperatures sufficiently below T_c two stable branches with amplitudes Q_{se} and Q_{sn} exist around which a simple semiclassical approximation is appropriate. For temperatures near T_c where $|\Lambda|$ is smaller than ϵ, the adequate semiclassical approximation depends on the particular values of the end points $\bar{r}$, x_i, and x_f in (104). Three cases must be distinguished. First, for $\bar{r}$, x_i, and x_f at most of order $\epsilon^{3/2}/\xi$ the eigenvalues $|\mathrm{Re}\{\Lambda_1(Q)\}|$ of the three complex branches of Q are smaller than ϵ and the quartic fluctuation potential $V(Q,Y_1)$ must be used. Similiarly to the static case ($x_i = x_f = 0$), one can show that the time-dependent density matrix is independent of the particular root of (104) that is inserted into (112). Second, for $\bar{r}$ smaller than order $\epsilon^{3/2}/\xi$ but x_i or/and x_f larger than order $\epsilon^{3/2}/\xi$, the eigenvalues $|\mathrm{Re}\{\Lambda_1(Q)\}|$ of Q_{se} and Q_{sn} become smaller than order ϵ while $\mathrm{Re}\{\Lambda_1(Q_u)\}$ is then larger than order ϵ and negative. Therefore, for fluctuations around the Q_{se} and Q_{sn} branches the quartic potential $V(Q,Y_1)$ is necessary and the density matrix is independent of the particular root Q_{se} or Q_{sn} inserted into $V(Q,Y_1)$. In

this region, the Q_u branch is well separated from the stable Q_{se} and Q_{sn} branches and its contribution to the path integral may be neglected since $\mathrm{Re}\{\Lambda_1(Q_u)\} < -\epsilon$. Finally, for end points $\bar{r}$ larger than order $\epsilon^{3/2}/\xi$, only the Q_{se} solution contributes and a simple semiclassical approximation of the fluctuation integral suffices. This is due to the fact that not only the contribution of the Q_u branch but also the contribution of the Q_{sn} branch is exponentially suppressed for $\mathrm{Re}\{\Lambda_1(Q_{sn})\} > -\epsilon$ since $\mathrm{Re}\{\xi^2\Sigma(Q_{sn})/i\epsilon^2\} - \mathrm{Re}\{\xi^2\Sigma(Q_{se})/i\epsilon^2\}$ is then larger than order 1. Here $\Sigma(Q)$ denotes the minimal effective action (85) evaluated at Q. The fluctuation prefactor (112) matches smoothly onto the simple semiclassical approximations for temperatures sufficiently below and above T_c.

Having evaluated the effective action and the fluctuation integral for small ξ and ϵ, we gain the time-dependent semiclassical density matrix

$$\rho(x_f, r_f, t) = \int dx_i\, dr_i\, d\bar{x}\, d\bar{r}\, J(x_f, r_f, t, x_i, r_i, \bar{x}, \bar{r}) \times \lambda(x_i, r_i, \bar{x}, \bar{r}) \tag{114}$$

with the propagating function

$$J(x_f, r_f, t, x_i, r_i, \bar{x}, \bar{r}) = \frac{1}{Z}\frac{\xi^3}{\epsilon^3}\frac{1}{8\pi|A(t)|}\frac{1}{\sqrt{4\pi\theta^2}}\left(\prod_{n=1}^{\infty}\nu_n^2\, u_n\right) K(Q) \times \exp\left\{\frac{i}{2}\frac{\xi^2}{\epsilon^2}\sum_{k=0}^{2}\xi^{k/2}[\Sigma_\theta^k(\bar{x},\bar{r}) + \Sigma_t^k(x_f, r_f, t, x_i, r_i, \bar{x}, \bar{r})]\right\}. \tag{115}$$

The contributions $\Sigma_\theta^k(\bar{x},\bar{r})$ to the imaginary time part of the minimal effective action Σ are given in (86), (90), and (97) while the contributions Σ_t^k to the real time part are specified in (89), (92), and (98). The fluctuation integral $K(Q)$ is specified in (112) and the amplitude Q may be calculated from the cubic equation (104). Within the semiclassical approximation the above formula (114) gives the time evolution of the density matrix near the top of a potential barrier starting from an initial state deviating from thermal equilibrium as described by the preparation function $\lambda(x_i, r_i, \bar{x}, \bar{r})$.

The formulas (114) and (115) are the central result of this article. Let us consider the range of temperature and time where the result (114) and (115) is valid. For temperatures $T < T_c$ the function Λ increases with increasing θ. As a consequence, the marginal mode amplitude Q also grows and terms in the minimal effective action, such as, e.g., $\xi^{3/2}r^3Q$, which are at most of order $\xi^{1/2}$ near T_c, become of order 1 for Λ of order $\xi^{1/6}$. Hence the result (114) is valid from high temperatures down to temperatures somewhat below T_c where Λ is still smaller than $\xi^{1/6}$.

Next let us discuss the range of time within which the above semiclassical density matrix is valid. The density matrix is evaluated by integrating the propagating function over initial coordinates. Hence an upper bound of time is provided by the condition that trajectories starting at $t = 0$ far away from the barrier top in the anharmonic range of the potential do not contribute to (114). This upper bound may be estimated by considering the case of vanishing damping. Then the energy of the relevant nonlocal paths is of the order of the potential energy at the barrier top since paths with larger energy are exponentially suppressed due to the Boltzmann factor in the propagating function while path with lower energy do not reach the barrier region. The time an undamped particle with an energy of order of the barrier height needs to reach the region near the barrier top when starting in the anharmonic range of the potential is determined by the long time behavior of the propagator $G_+(t)$. According to (I83), for times $t \gg 1$ one has an exponential growth as $G_+(t) \propto \exp(t)$ in the undamped case. Hence the time t to reach end points within a region at most of order $\xi^{-1/4}$ about the barrier top when starting from initial coordinates of order $1/\xi$ with an energy of order of the barrier height is at least of order $|\ln\xi|$. For nonvanishing damping the long time behavior of $G_+(t)$ is given by $\exp(\omega_R t)$, where ω_R is the Grote-Hynes frequency [14] given by the positive solution of $\omega_R^2 + \omega_R\hat{\gamma}(\omega_R) = 1$. As a consequence, for nonvanishing damping the upper bound of time can be estimated as $t \ll \omega_R^{-1}|\ln\xi|$.

We note that another upper bound of time arises from the fact that we evaluate the time evolution of the density matrix near the instability point of an anharmonic potential. Correspondingly, the equilibrium density matrix increases with increasing coordinate $\bar{r}$. This coordinate is connected to the initial coordinates x_i and r_i of the real time trajectories via the preparation function $\lambda(x_i, r_i, \bar{x}, \bar{r})$. Hence, depending on the preparation function, the domain of relevant coordinates x_i, r_i, and $\bar{r}$, which contribute to the integrals in (114), may also increase with increasing time and eventually may become larger than the barrier region where our results are valid. In summary, the semiclassical density matrix (114) is valid for high temperatures down to temperatures somewhat below T_c, for end coordinates at most of order $\xi^{-1/4}$, and for a large time range with an upper bound of order $\omega_R^{-1}|\ln\xi|$.

C. Equilibrium density matrix

For $t = 0$ the density matrix (1) reduces to the initial state (2). Here we want to recover this result from (115). In particular, for the preparation function $\lambda(x_i, r_i, \bar{x}, \bar{r}) = \delta(x_i - \bar{x})\,\delta(r_i - \bar{r})$, the initial state reduces to the equilibrium density matrix of the dissipative quantum system.

In the limit $t \to 0$, the functions $A(t)$ and $S(t)$ can be expanded according to (I71) and (I72) as

$$A(t) = -\frac{t}{2} + O(t^3) \tag{116}$$

and

$$S(t) = \Lambda - \frac{1}{2}\Omega t^2 + O(t^4). \tag{117}$$

Correspondingly, the functions $F_3^{\alpha}(t)$, $C_{1,\alpha}(t)$, and $I_{\alpha,0}(t,0)$, as well as $C_1^{+}(t)$ appearing in the cubic equation (104), vanish for $t \to 0$ and the amplitude Q becomes a time-independent function of $\bar{r}$ only, which will be denoted by $\bar{Q}$. The real time part of the minimal effective action reduces according to (116) and (117) to

$$\sum_{k=0}^{2} \xi^{k/2}\, \Sigma_t^k(x_f, r_f, t, x_i, r_i, \bar{x}, \bar{r}) = \frac{(x_f - x_i)(r_f - r_i)}{t} - \frac{i}{2}\Omega x_i^2 + \frac{i}{2}\Omega x_f^2 + O(t). \tag{118}$$

This combines with the imaginary time part of the minimal effective action (86), (90), and (97) to yield the propagating function (115) for small times

$$J(x_f, r_f, t, x_i, r_i, \bar{x}, \bar{r}) = \frac{1}{Z}\frac{\xi^3}{\epsilon^3}\frac{1}{\sqrt{4\pi\theta^2}}\left(\prod_{n=1}^{\infty}\nu_n^2 u_n\right) K(\bar{Q}) \exp\left[\frac{i}{2}\frac{\xi^2}{\epsilon^2}S_\theta(\bar{x},\bar{r})\right]\frac{1}{4\pi t}\exp\left\{\frac{i}{2}\frac{\xi^2}{\epsilon^2}\left[\frac{(x_f - x_i)(r_f - r_i)}{t} - \Omega x_i^2 + \Omega x_f^2\right]\right\}, \tag{119}$$

where

$$S_\theta(\bar{x},\bar{r}) = \sum_{k=0}^{2}\xi^{k/2}\,\Sigma_\theta^k(\bar{x},\bar{r})\Big|_{x(s)=0}. \tag{120}$$

The time-dependent part in (119) represents, for $t \to 0$, the δ functions $\delta(x_f - x_i)\,\delta(r_f - r_i)$ and we have

$$\lim_{t\to 0} J(x_f, r_f, t, x_i, r_i, \bar{x}, \bar{r}) = \delta(x_f - x_i)\delta(r_f - r_i)\,\rho_\theta(\bar{x},\bar{r}). \tag{121}$$

This way we obtain from (114), in the limit $t \to 0$, the expected result

$$\rho(x_f, r_f, 0) = \int d\bar{x}\, d\bar{r}\, \lambda(x_f, r_f, \bar{x}, \bar{r})\rho_\theta(\bar{x},\bar{r}), \tag{122}$$

where the dimensionless equilibrium density matrix for temperatures near T_c reads

$$\rho_\theta(\bar{x},\bar{r}) = \frac{1}{Z}\frac{\xi}{\epsilon}\frac{1}{\sqrt{4\pi\theta^2}}\left(\prod_{n=1}^{\infty}\nu_n^2 u_n\right) K(\bar{Q}) \times \exp\left[\frac{i}{2}\frac{\xi^2}{\epsilon^2}S_\theta(\bar{x},\bar{r})\right]. \tag{123}$$

Here Z is a normalization constant and $\bar{Q}$ is determined by the cubic equation (104) for $x_i = x_f = 0$, i.e.,

$$\frac{\Lambda}{\xi^{1/2}}\bar{Q} - 2\theta^3 c_4 D_4(1 - \theta\Lambda)\,\xi^{1/2}\bar{Q}^3 - 3c_4\theta^2 D_3\,\xi\bar{Q}^2\bar{r} = \frac{\bar{r}}{2\theta}. \tag{124}$$

According to (120), the minimal imaginary time action reads

$$S_\theta(\bar{x},\bar{r}) = i\left[\theta\frac{\bar{Q}\bar{r}}{\xi^{1/2}} + \frac{\Omega}{2}\bar{x}^2 - c_4\theta^4\left(2\theta D_4\bar{Q}^4 + 4D_3\,\xi^{1/2}\bar{r}\bar{Q}^3 + \frac{3}{\theta}D_2\,\xi\bar{r}^2\bar{Q}^2\right) + 32c_6\theta^6\left(D_5\,\xi^{3/2}\bar{r}\bar{Q}^5 + \frac{\theta}{3}D_6\,\xi\bar{Q}^6\right)\right] + O(\xi^{1/2}). \tag{125}$$

For temperatures above the critical temperature where $|\Lambda|$ is larger than order $\xi^{1/2}$, (125) reduces to the harmonic action (91) and from (123) one regains, in this limit, the equilibrium density matrix of a damped, inverted harmonic oscillator (I78). For vanishing damping the equilibrium density matrix (123) coincides in leading order in ξ with our earlier result [10]. Hence (123) generalizes the investigation of [10] to dissipative quantum systems.

VII. SUMMARY AND ILLUSTRATION OF RESULTS AND CONCLUSIONS

In this section we summarize the main results and clarify the interrelationship between the various formulas derived. The results are illustrated with an example.

A. Explicit evaluation of the density matrix

To obtain definite results for the density matrix the propagating function (115) has to be evaluated explicitly. This is done in the following way. For a system with given dissipative mechanism the macroscopic damping kernel $\gamma(s)$ or its Laplace transform $\hat{\gamma}(z)$ is known. At given inverse temperature θ and time t, five basic functions can be evaluated. Three of these are Λ, defined in (9) with (13), which vanishes at $\theta = \theta_c$; Ω defined in (103); and the marginal direction in function space $\phi(\sigma)$

defined in (23) with (13) and (21). Since $\phi(\sigma)$ is needed in the time interval $(0,\theta)$ only, it is convenient to use the representation (15) for explicit evaluations. The functions Λ, Ω, and $\phi(\sigma)$ are characteristic for the imaginary time motion. The two other functions are $A(t)$, defined in (87) with (60), and $S(t)$, defined in (88) with (30), (50), and (63). These functions are characteristic for the real time motion. We note that, apart from $\phi(\sigma)$, these functions are already needed to determine the propagating function (I80) for the purely harmonic potential.

From $\phi(\sigma)$ one obtains in the next step the coefficients D_n defined in (37). For the contributions Σ_θ^1 and Σ_θ^2 to the imaginary time part of the minimal effective action the coefficients $D_2,\ldots,D_6$ are needed, while the real time parts Σ_t^1 and Σ_t^2 depend on D_4 only. Due to the fact that the functions $C_n^+(t)$ can be expressed in terms of $A(t)$ and $S(t)$ [see (102)], these latter functions determine $I_{\alpha,n}(t,s)$ in (71), which is needed for $n=0,1$, the functions $j_\alpha(t)$ in (84), $j_\alpha^+(t)$ in (100), and $C_{\alpha,n}(t)$ in (93). Further, from these functions and $\gamma(s)$, the functions $\gamma_\alpha(t)$ and $\gamma_{\alpha,\beta}(t)$ introduced in (83) and (101), respectively, may be evaluated. Finally, the functions $F_p^{\alpha_1\cdots\alpha_m}(t)$ in (96), which are needed for $p=2,3,5$ and $m=1,2$, are determined by $A(t)$, $\gamma(s)$, and $\phi(\sigma)$. These functions describe higher-order couplings between the real time and imaginary time motion. So far all functions are specific for the dissipative mechanism and independent of the form of the potential barrier.

The marginal mode amplitude Q is determined by the cubic equation (104), which contains the functions $A(t)$, $S(t)$, $I_{\alpha,0}(t,0)$, $C_{\alpha,1}(t)$, and $F_3^\alpha(t)$. This equation also depends on potential parameters. Having solved the cubic equation (104) for Q at given inverse temperature θ and coordinates $\bar r$, x_f, and x_i, the minimal effective action (85) can be calculated for given coordinates x_f, r_f, x_i, r_i, $\bar x$, and $\bar r$. All coefficients of the fluctuation potential are now known and the fluctuation integral $K(Q)$ can be determined from (112). Then the propagating function is known explictly. Finally, with an appropriate preparation function $\lambda(x_i,r_i,\bar x,\bar r)$, one gets the density matrix (114).

B. The quartic potential with Ohmic dissipation

To illustrate the above results we investigate the time evolution of a particle that is initially localized near the barrier top of the quartic potential field

$$V(q)=-\frac{1}{2}q^2+\frac{1}{4}\xi^2 q^4. \tag{126}$$

This model is obtained by setting $c_4=1$ and $c_{2k}=0$ for $k>2$ in the above formulas. The heat bath is chosen to be Ohmic leading to frequency-independent damping. Then the macroscopic damping kernel reads $\gamma(t)=2\gamma\delta(t)$ and its Laplace transform $\hat\gamma(z)=\gamma$. This allows for an explicit evaluation of some functions involved in the propagating function. One gets

$$\Lambda=-\frac{1}{\theta}+\frac{1}{(2\omega_R+\gamma)\pi}\times\left[\Psi\left(1+\frac{\omega_R+\gamma}{\nu_1}\right)-\Psi\left(1+\frac{\omega_R}{\nu_1}\right)\right], \tag{127}$$

where $\Psi(x)$ denotes the digamma function and

$$\omega_R=\left(\frac{\gamma^2}{4}+1\right)^{1/2}-\frac{\gamma}{2}. \tag{128}$$

The temperature-dependent function Ω given in (103) has a logarithmic divergency for Ohmic damping. This can be removed by introducing a more realistic damping kernel with finite memory time such as, e.g., in a Drude model where $\gamma(t)=\gamma\omega_D\exp(-\omega_D t)$ and $\hat\gamma(z)=\gamma\omega_D/(\omega_D+z)$. In the limit $\omega_D\gg 1,\gamma$ the Drude model behaves like an Ohmic model except for very short times of order $1/\omega_D$, which we do not consider here. Accordingly, we get from (103)

$$\Omega=\frac{1}{\theta}\sum_{n=-\infty}^{\infty}\frac{|\nu_n|\gamma\omega_D/(\omega_D+|\nu_n|)-1}{\nu_n^2+|\nu_n|\gamma\omega_D/(\omega_D+|\nu_n|)-1}. \tag{129}$$

The basic time-dependent functions are obtained as [6]

$$A(t)=\frac{1}{2}\frac{1}{2\omega_R+\gamma}\{\exp[-(\omega_R+\gamma)t]-\exp[\omega_R t]\} \tag{130}$$

and

$$S(t)=-\frac{1}{2}\frac{1}{2\omega_R+\gamma}\left\{\cot\left(\frac{\omega_R+\gamma}{2}\theta\right)\exp[-(\omega_R+\gamma)t]+\cot\left(\frac{\omega_R}{2}\theta\right)\exp[\omega_R t]\right\}-\Gamma(t), \tag{131}$$

where

$$\Gamma(t)=\frac{2\gamma}{\theta}\sum_{n=1}^{\infty}\frac{\nu_n\exp(-\nu_n t)}{(\nu_n^2-1)^2-\gamma^2\nu_n^2}$$

$$=-\frac{1}{2\omega_R+\gamma}\left\{\frac{1}{\omega_R}\left[{}_2F_1\left(1,\frac{\omega_R}{\nu_1},1+\frac{\omega_R}{\nu_1};e^{-\nu_1 t}\right)-{}_2F_1\left(1,-\frac{\omega_R}{\nu_1},1-\frac{\omega_R}{\nu_1};e^{-\nu_1 t}\right)\right]\right.$$

$$\left.-\frac{1}{\omega_R+\gamma}\left[{}_2F_1\left(1,\frac{\omega_R+\gamma}{\nu_1},1+\frac{\omega_R+\gamma}{\nu_1};e^{-\nu_1 t}\right)-{}_2F_1\left(1,-\frac{\omega_R+\gamma}{\nu_1},1-\frac{\omega_R+\gamma}{\nu_1};e^{-\nu_1 t}\right)\right]\right\} \tag{132}$$

with the hypergeometric function ${}_2F_1(a,b,c;z)$. Furthermore, from (30) we gain

$$g_n(s) = 2\gamma\delta(s) - |\nu_n|\gamma \exp(-|\nu_n|s). \tag{133}$$

Now let us consider the preparation function

$$\lambda(x_i,r_i,\bar{x},\bar{r}) = \delta(x_i-\bar{x})\,\delta(r_i-\bar{r})\,\frac{1}{\sqrt{4\pi\sigma_0}} \times \exp\left[-\frac{(r_i-q_0)^2}{4\sigma_0} - \frac{x_i^2}{16\sigma_0}\right] \Big/ \rho_\theta(\bar{x},\bar{r}), \tag{134}$$

which describes an initial state where the particle is localized near q_0. Here $\rho_\theta(\bar{x},\bar{r})$ is the equilibrium density matrix (123) with $c_6 = 0$. The diagonal part of the initial reduced density matrix is a Gaussian wave packet independent of temperature and reads

$$P(q,0) = \frac{1}{\sqrt{4\pi\sigma_0}} \exp\left[-\frac{(q-q_0)^2}{4\sigma_0}\right]. \tag{135}$$

We are interested in the position probability distribution $P(q,t) = \rho(0,q,t)$ describing the decay of the unstable initial state. Inserting (134) into (114) one gains

$$P(q,t) = \frac{1}{\sqrt{4\pi\sigma_0}} \int dx_i\, dr_i\, J(0,q,t,x_i,r_i,x_i,r_i) \times \exp\left[-\frac{(r_i-q_0)^2}{4\sigma_0} - \frac{x_i^2}{16\sigma_0}\right] \Big/ \rho_\theta(x_i,r_i). \tag{136}$$

Proceeding along the lines described in Sec. VII A, $P(q,t)$ may be determined explicitly. Some results are illustrated in Fig. 2. The position distribution function $P(q,t)$ is shown for various times t and for Ohmic damping with $\gamma = 5$. The cutoff that regularizes Ω in (129) is chosen to be $\omega_D = 100$. Hence the dynamics of the system behaves like that of an Ohmic model for times $t \gg 0.01$. From (127) one obtains, for $\gamma = 5$, the critical inverse temperature $\theta_c = 6.289\ldots$. Further, we have chosen $\xi = \epsilon = 0.05$, $\sigma_0 = 0.02$, and $q_0 = 0.04$, which allows to study the decay of the unstable initial state for times up to $t \approx 10$. Figure 2(a) represents $P(q,t)$ for small inverse temperatures $\theta = 1$, while Fig. 2(b) depicts results for $\theta = \theta_c$. Thermal and quantum fluctuations lead to a decay of the initial state causing a decrease of the maximum of the distribution function and an increase of the width with increasing time. However, a doubly peaked distribution emerges at larger times when the system reaches the nonlinear range of the potential. This occurs sooner at lower temperatures [Fig. 2(b)], where quantum fluctuations are large.

To study this point in greater detail we determine the probabilities to find particles on the left- or the right-hand side of the barrier, respectively. These probabilities are given by

$$p_\pm(t) = \int dq\, P(q,t)\,\Theta(\pm q), \tag{137}$$

with $p_+(t) + p_-(t) = 1$. In particular, for $t = 0$ we gain,

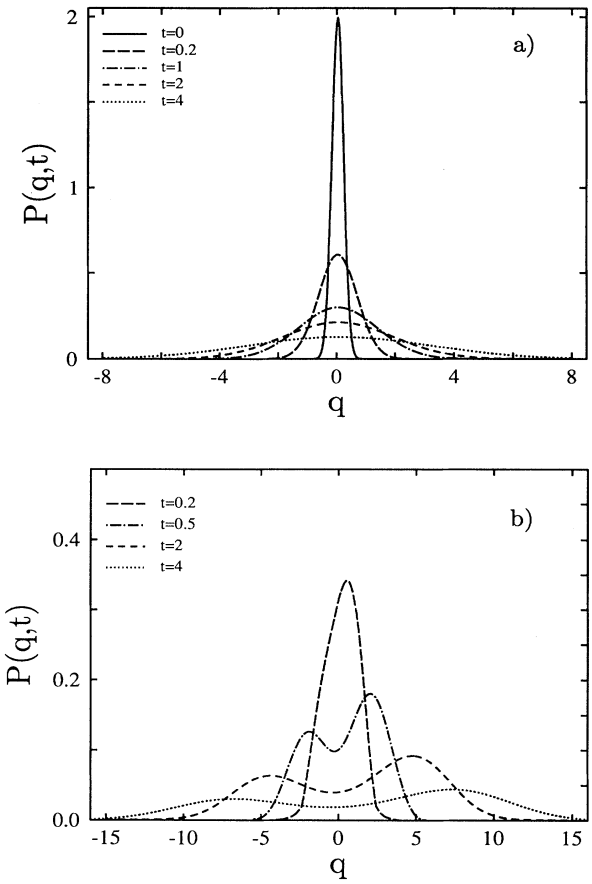

FIG. 2. Position distribution function $P(q,t)$ for a system with a quartic potential and Ohmic dissipation starting from the unstable initial state (134) for various times t and (a) $\theta = 1.0$ and (b) $\theta = \theta_c = 6.2895$. See the text for system parameters.

from (135) and (137),

$$p_-(0) = \frac{1}{2}\mathrm{erfc}\,(q_0/2\sqrt{\sigma_0}), \tag{138}$$

where $\mathrm{erfc}(z)$ denotes the complement to the error function. For large times $p_\pm(t)$ become stationary and the splitting ratio $r(t) = p_-(t)/p_+(t)$ saturates at a finite value r_s.

In particular, for the case of a purely parabolic barrier, the integrals in (136) and (137) can be done exactly. Then, one obtains

$$p_-^{\mathrm{PB}}(t) = \frac{1}{2}\mathrm{erfc}\left\{\frac{q_0}{2}\left[\frac{A(t)^2\Lambda^2}{S(t)^2\sigma_0}(1-4\sigma_0\Omega) + \sigma_0 - \Lambda + \frac{\Lambda^3}{S(t)^2}\right]^{-1/2}\right\}. \tag{139}$$

The high-temperature limit of this formula leads to the classical result, which reads for large times

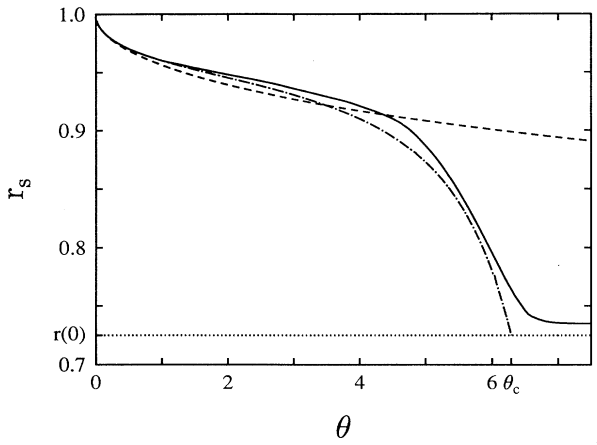

FIG. 3. Asymptotic value of the splitting ratio r_s of an unstable initial state as a function of inverse temperature θ. See the text for system parameters. The solid line represents the result for the quartic potential, the dashed line represents the classical result, and the dash-dotted line represents the quantum mechanical result for a parabolic potential. The initial value of the splitting ratio $r(0)$ is shown as a dotted line.

$$\lim_{\omega_R t \gg 1} p_-^{\rm cl}(t) = \frac{1}{2}\mathrm{erfc}\left[\frac{q_0}{2}\left(\frac{\theta}{1-\omega_R^2+\theta\sigma_0}\right)^{1/2}\right]. \quad (140)$$

Figure 3 shows the asymptotic value r_s of the splitting ratio for the quartic potential as well as the quantum mechanical and the classical results for the purely parabolic barrier as a function of the inverse temperature θ. We have used the same set of parameters as above. In this case the ratio $r(t)$ becomes independent of time for $t \gtrsim 4$. For high temperatures the system behaves classically. Then a decrease of temperature leads to a decrease of thermal fluctuations so that r_s also decreases. At lower temperatures quantum effects are important. First, due to the small width σ_0 of the initial position distribution $P(q,0)$, momentum fluctuations enhance r_s above the classical value. On the other hand, due to tunneling processes, the width of the minimum of the diagonal part of the equilibrium density matrix $P_\theta(q)$ at the barrier top becomes smaller than that of the classical distribution. This corresponds effectively to a barrier with larger curvature leading to a smaller ratio r_s. The first effect dominates in an intermediate temperature range, while the second effect dominates for low temperatures near θ_c. For a purely parabolic barrier the width of the minimum of $P_\theta(q)$ is proportional to $\sqrt{|\Lambda|}$, which decreases with increasing inverse temperature and vanishes at θ_c so that then $r_s = r(0)$ [see also (139)]. In the quartic barrier potential the value of r_s decreases rapidly within a narrow temperature region around θ_c and then settles at a value of r_s somewhat above $r(0)$. For inverse temperatures $\theta > \theta_c$ the splitting ratio r_s becomes nearly independent of temperature. This demonstrates again that the change of stability of the minimal action paths and the breakdown of the simple semiclassical approximation near T_c correspond to a changeover from a temperature range where the dynamics near the barrier top is almost classical to a range where quantum effects dominate.

C. Conclusions

Employing the path integral approach, we have calculated the density matrix of a dissipative quantum system with a general anharmonic and symmetric barrier in the temperature region where large quantum fluctuations near the barrier top render the harmonic approximation insufficient. We have shown that for a weakly anharmonic potential, where the ground state in the inverted potential is only weakly affected by anharmonicities, the time evolution of the density matrix can be determined by means of classical perturbation theory and the semiclassical approximation.

Near a critical temperature T_c, one mode of the imaginary time path fluctuations becomes marginal in the purely harmonic potential; however, due to anharmonicities, the corresponding amplitude remains finite near T_c. The fluctuation path integral has to be determined beyond the Gaussian approximation in this critical region. Due to the damping-induced coupling between the imaginary and the real time motion, the real time paths are also affected by anharmonic terms in the potential field.

Within the systematic approximations made, controlled by the small anharmonicity parameter ξ and the small parameter ϵ for quantum fluctuations, the results on the time evolution of the density matrix are valid from high temperatures down to temperatures somewhat below T_c and over a large range of time excluding very long times. The approximation scheme advanced in this article can formally be extended also to temperatures far below T_c, however, an explicit evaluation of the density matrix then requires numerical methods. We have illustrated our results by considering the dynamics of a particle initially localized near the instability point of a quartic model potential. The findings of this article may also be used to determine a quasistationary nonequilibrium flux state. This extension of results presented in I to the temperature region where quantum tunneling is dominant is planned to be given in a subsequent paper.

ACKNOWLEDGMENTS

The authors would like to thank G.-L. Ingold and F.J. Weiper for helpful discussions. This work was supported by the Deutsche Forschungsgemeinschaft (Bonn).

[1] P. Hänggi, P. Talkner, and M. Borkovec, Rev. Mod. Phys. **62**, 251 (1990), and references therein.
[2] J. Ankerhold, H. Grabert, and G.-L. Ingold, Phys. Rev. E **51**, 4267 (1995), referred to as I in the following.
[3] R. P. Feynman and F. L. Vernon, Ann. Phys. (N.Y.) **243**, 118 (1963).
[4] R. P. Feynman and A. P. Hibbs, *Quantum Mechanics and Path Integrals* (McGraw-Hill, New York, 1965); R. P. Feynman, *Statistical Mechanics* (Benjamin, New York, 1972).
[5] A. O. Caldeira and A. J. Leggett, Phys. Rev. Lett. **46**, 211 (1981); Ann. Phys. (N.Y.) **149**, 374 (1983); **153**, 445(E) (1984).
[6] H. Grabert, P. Schramm, and G.-L. Ingold, Phys. Rep. **168**, 115 (1988).
[7] U. Weiss, *Quantum Dissipative Systems* (World Scientific, Singapore, 1993).
[8] H. Grabert, P. Olschowski, and U. Weiss, Phys. Rev. B **36**, 1931 (1987), and references therein.
[9] L. S. Schulman, *Techniques and Applications of Path Integrals* (Wiley, New York, 1981).
[10] J. Ankerhold and H. Grabert, Physica A **188**, 568 (1992).
[11] F. J. Weiper, J. Ankerhold, and H. Grabert (unpublished).
[12] J. Ankerhold, Ph.D. thesis, University of Essen, 1994 (unpublished).
[13] We refer to Eq. (x) in I (Ref. [2]) as (Ix).
[14] R. F. Grote and J. T. Hynes, J. Chem. Phys. **73**, 2715 (1980); P. Hänggi and F. Mojtabai, Phys. Rev. A **26**, 1168 (1982).